Journal of
Chemical Engineering Research & Reviews

Allenbrand C. J Chem Eng Re Rev: JCERR-101
Doi.org/10.47378/JCERR/2022.1.100101

Research Article Open Access

Correlational Analysis of Binary Distillation Using Experimental, Mathematical, and Computational Methods for Process Design Information

Corban Allenbrand*

Chemical and Petroleum Engineering, The University of Kansas, Lawrence, United States.

Abstract

The design of distillation processes must satisfy several requirements - controllability, safety, operability, and economic productivity – that are determined from experimentation, mathematical modeling, and computational simulation. This work investigated the relation between column variables and the mole fraction of methanol (MeOH) in the distillate stream (x_D) on a modified Oldershaw column under semi-automatic control to capture column operating behavior. A positive correlation between the MeOH x_D and reflux ratio was found. A rigorous RadFrac model from the Aspen Plus V10 software simulated an analogous relationship. The percent mean absolute error (MAE) between the model predictions and experimental observations was 1%. A correlation between the feed flow rate and the MeOH x_D was also discovered with a comparison between Aspen Plus predictions and empirical measurements that resulted in a percent MAE of 3%. This information was utilized to design a feasible economic solution for the separation of a 50:50 MeOH isopropanol mixture. This solution consisted of sequential distillation columns. It was found that salaries and utilities were the dominant contributor to total liabilities, a result of transient operating hours. This study demonstrated how merged experimental and model information can be integrated and used to gain access to insights into the design of complex design projects.

Keywords: *distillation simulation; distillation experiment; distillation model; distillation design; distillation economics; distillation aspen plus.*

Introduction

Distillation is one of the most predominant and widely studied separation technique used in the chemical process industry. Due to factors such as high mass transfer rates, when separation is feasible, distillation is regarded as one of the most effective means to achieve separation [1]. The advantages of distillation including economics of scale, well-established technologies, competitive supply of equipment, high purity products, and energy integration opportunities encourage continued optimization of distillation operations [2]. Although it represents an effective technique to achieve separation, distillation is energy intensive. It has been estimated that 6% of all U.S. domestic energy use and 24% of the total U.S. industrial energy use is attributable to the chemical industry. Of that, separations are estimated to account for 60% of the in-plant energy usage for the chemical industry with distillation operations accounting for approximately 95% of the total separation energy usage [3]. In 2021, the industrial sector accounted for 33% of total U.S. energy consumption representing 32.12 quadrillion British thermal units. Using estimates from the U.S. Department of Energy (2005) [3], in 2021, roughly 4.5% of the total U.S. energy consumption was due to distillation operations. Improvements to the energy efficiency and separation effectiveness of distillation is the focus of many studies including in reactive distillation, internally heat-integrated distillation, dividing-wall columns, and multiple phase division distillation [4-7]. Currently, these promising alternatives to conventional columns are used for specific applications such as the use of dividing wall columns to affect the separation of three product streams in a single column [8].

The performance of the distillation column, in terms of the degree of separation of the components and the purity of the product stream, is dependent on several factors such as operating variables (reflux rate, feed flow rate, etc.), column internals (tray type, tray geometry, etc.), column size, hydraulic phenomena and the physical and chemical properties of the components [9]. It is common for the engineer to utilize software such as ASPEN Plus to model a distillation through two modes of modelling, design and rating. The development of a predictive distillation model, one that can explain empirical observations and forecast future changes in operating conditions, is valuable to the chemical process industry [10]. This work addressed the rating mode of modelling where the column configuration existed and its operation envelope was to be explored. Empirical measurements of the column operation were assimilated with computer simulations using ASPEN Plus software model predictions to determine the column performance and to establish a predictive understanding of

***Corresponding author:** Corban Allenbrand, Chemical and Petroleum Engineering, The University of Kansas, Lawrence, United States. 1127 Klein Ct. Lawrence, KS, 66049, Tel: 1-913-963-2669; Email: callenbrand@ku.edu

Citation: Allenbrand C (2022) Correlational Analysis of Binary Distillation Using Experimental, Mathematical, and Computational Methods for Process Design Information. J Chem Eng Re Rev: JCERR-101.

Received Date: August 11th, 2022; **Accepted Date:** August 18th, 2022; **Published Date:** August 25th, 2022

the relationship between two operating variables - reflux ratio and feed volumetric flow rate – to the separation performance of the column – distillate product mole fraction. This information, combined with background knowledge, was employed to design, plan, and implement a model company tasked with separating the binary system of methanol and isopropanol.

Theoretical Background

Separation by distillation can be approached and analyzed as an equilibrium-based mechanism. A tractable analytical evaluation of a distillation column and the derivation of closed-form expressions for mass and energy balances demands several assumptions regarding the equilibrium stage concept, constant relative volatility, and constant molar flow rates [11].

The first of these assumptions, the equilibrium or theoretical stage concept, is pervasive in the theory of distillation [12]. This assumes that the liquid and vapor leaving a tray are in stable VLE which presupposes perfect mixing of the components. Interfacial mass and energy transfer - rate-based events - are ignored as these require direct mathematical modelling of the individual stages. Instead, only a good description of VLE is necessary for practical evaluation of the column [13]. The formation of VLE is achieved with counter-current flows of vapor (v) and liquid (l) that enables equilibration of the phases and components. For any binary system with two phases at VLE, three conditions must hold where T is the temperature, P is the pressure, and G is the partial molar Gibbs free energy [2].

- Thermal equilibrium, $T^v = T^l$
- Mechanical equilibrium, $P^v = P^l$
- Chemical equilibrium, $\bar{G}_i^v = \bar{G}_i^l$.

Chemical equilibrium with equalities of G can be stated as an equality of fugacities. Fugacity can be thought of as the tendency of a component in one phase to escape into another phase. Hence, at equilibrium, each component in a mixture must have equal tendency to escape between phases [14]. At VLE then, it must be true that the vapor and liquid phase fugacities (f) must be equivalent for each component (i) as expressed in an iso-fugacity relation (1) where θ is the fugacity coefficient, y is the vapor mole fraction, x is the liquid mole fraction, γ is the activity coefficient, V is molar volume and R is the gas constant. If this were not the case, then the component with greater fugacity would move into whatever phase lowered its chemical potential, making analytic expression like (1) unavailable [15]. The general expression for VLE given by (1) is assuming a vapor mixture and a liquid solution.

$$f_i^v = f_i^l \Rightarrow \hat{\theta}_i^v(T,P) y_i P = \gamma_i x_i \theta_i^{sat} P_i^{vap} e^{\left[V_i\left(\frac{P-P_i^{vap}}{RT}\right)\right]}. \quad (1)$$

Note that (1) can be reduced to a more tractable form with a few assumptions' additional assumptions. First, the absence of strong chemical and physical forces and system temperatures and pressures that are far from the critical points of both components result in θ = 1 for both phases. Second, a low system pressure near the vapor pressure of the liquid allows the exponential term to go to one. With these, (1) simplifies to (2)

$$y_i P = \gamma_i x_i P_i^{vap}. \quad (2)$$

Another assumption is constant relative volatility between components i and j (α_{ij}). Relative volatility depends upon the ratio of K-values for the components given by: K_i/K_j and with the K-values defined as: $K_i = y_i/x_i$. For ideal mixtures that satisfy Raoult's law, (3) provides a useful expression [13].

$$\alpha_{ij} = \frac{K_i}{K_j} = \frac{y_i/x_i}{y_j/x_j} = \frac{y_i(1-x_i)}{x_i(1-y_i)} = \frac{P_i^{vap}}{P_j^{vap}} \quad (3)$$

It is standard to define an average column-wise relative volatility that is the geometric mean of the relative volatiles at the top and bottom of a column segment. This value becomes relevant in column efficiency calculations such as in the computation of the O' Connell tray efficiency given by (4) where μ is the feed viscosity.

$$Tray\ Efficiency, \eta = 50.3(\alpha\mu)^{-0.226} \quad (4)$$

In addition to the tray efficiency, a column efficiency is computable from (5) where N_T denotes the number of theoretical trays, a value returned from shortcut methods, and N_{act} indicates the actual number of trays in a distillation column [16].

$$Column\ Efficiency, E_o = \frac{N_T}{N_{act}} \quad (5)$$

The above assumptions result in a mathematical model for a distillation column where each equilibrium stage or tray, depicted in Figure 1, of the column satisfies four equations known as the MESH equations-mass balance (M), phase equilibrium relations (E), mole fraction summation relations (S), energy balance (H)-which are used to obtain thermodynamic profiles within the column [17]. From Figure 1 and ignoring side vapor and liquid streams SV and SL, the MESH equations are specified by (6)-(10), respectively [18].

First, for stage *j*, a mass balance relation (6) requires the all mass into and out of a stage is conserved

$$L_{j-1} + V_{j+1} + F_j = L_j + V_j + SV_j + SL_j. \quad (6)$$

With mole fractions of component *i* in stage *j*, a mole balance is described in (7) whereby the number of moles is conserved across a stage

$$L_{j-1}x_{i,j-1} + V_{j+1}y_{i,j+1} + F_j z_{i,j} = L_j x_{i,j} + V_j y_{i,j} + SL_j x_{i,j} + SV_j y_{i,j} \quad (7)$$

With the K value, or equilibrium ratio, which quantifies the mole fraction in one phase to that in another, the phase equilibrium relation of (1) can be written from Raoult's Law as,

$$y_{i,j} - K_{i,j}x_{ij} = 0. \quad (8)$$

The assumption of VLE at stage *j* allows a molar summation relation (9) which states that all liquid or vapor at a stage *j* must be represented in either the liquid or vapor phase

$$\sum_{i=1}^{C}(x_{i,j} - y_{i,j}) = 0 \quad (9)$$

Last, provided there are no changes in kinetic or potential energies (gravitational, electromagnetic) then an energy balance at stage *j* is given in (10)

$$L_{j-1}H_{j-1}^{L} + V_{j+1}H_{j+1}^{V} + F_j H_j^{F} = L_j H_j^{L} + V_j H_j^{V} + SV_j H_j^{V} + SL_j H_j^{L} + Q_j \quad (10)$$

where H_j^F, H_j^V, H_j^L are the enthalpies of the feed, vapor, and liquid, Q_j is energy exchange with the environment, SV_j and liquid SL_j denote the side vapor and side liquid streams. Interested readers are directed to Steffen et al. (2016) [17] and Schaschke (2014) [19] for further details on the MESH relations.

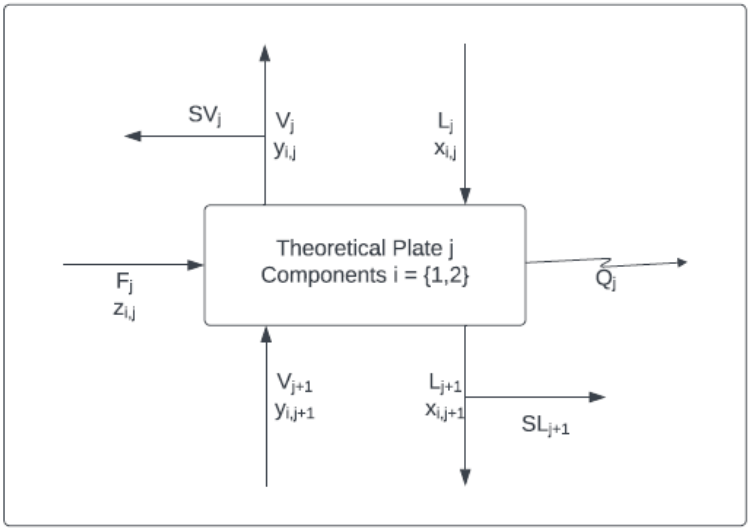

Figure 1: Equilibrium tray mathematical model where F = feed molar flow rate, L = liquid molar flow rate, V = vapor molar flow rate, z = feed mole fraction, y = vapor mole fraction, x = liquid mole fraction and Q are heat supplies or losses on a tray. For binary separation, there are two components and so i=1,2.

McCabe-Thiele Method

The McCabe-Thiele method is a simple model of distillation that, when followed, yields a graphical tool called the McCabe-Thiele plot that returns the number of theoretical trays of a column [20]. The method is predicated on four assumptions:

- Binary mixture
- Heats of vaporization are the same for each component
- Enthalpy of mixing, heat of solvation and other thermodynamic effects are ignorable
- 100% tray efficiency

The construction of the McCabe-Thiele plot requires several information categories including VLE data, feed composition, temperature of the feed and composition of the top and bottom products [21]. With the graphical tool developed, tedious calculations can be bypassed and quick judgements on design choices can be reached. Inspiration from the McCabe-Thiele method has resulted in the development of mathematical programming approaches to column design [22]. Graphical methods like the MCabe-Thiele are critical tolls in the preliminary and conceptual phases of design. Other graphical methods such as the

Ponchon-Savarit method exist to aid in distillation design [23]. It was pointed out by a Reviewer that the graphical method employed in the McCabe-Thiele method bears similarity to a mechanism adopted in coordinated control.

Completion of the method consists of plotting three lines on the equilibrium diagram for a binary system. The first line models the rectifying section of the column and from knowing the constant liquid flow rate for tray *n* in the rectifying section (L_n^R), constant vapor flow rate for tray *n+1* in the rectifying section (V_{n+1}^R), distillate flow rate (D), reflux ratio (R) = L/D, liquid molar composition for tray *n* in the rectifying section (x_n^R) and distillate molar composition (x_D), a user can go from a material balance for the rectifying section given by (11) to the linear equation for the rectifying section operating line (ROL) declared in (12) where (y_{n+1}^R) denotes the vapor molar composition in tray *n+1* in the rectifying section.

$$V_{n+1}^R y_{n+1}^R = L_n^R x_n^R + D x_D \quad (11)$$

$$y_{n+1} = \frac{R}{R+1} x_n + \frac{1}{R+1} x_D \quad (12)$$

A material balance around the stripping section is given by (13) where knowledge of the bottoms flow rate (B), bottoms molar composition (x_B), molar composition of the liquid in tray *n* in the stripping section (x_n^S), liquid flow rate in tray *n* in the stripping section (L_m^S), vapor flow rate in tray *n+1* in the stripping section (V_{n+1}^S) can be used to calculate the stripping section operating line (SOL) given by (14). The SOL is used to compute the vapor molar composition in tray *m* (y_{m+1}).

$$L_n^S x_n^S = V_{n+1}^S y_{n+1}^S + B x_B \quad (13)$$

$$y_{n+1}^S = \frac{L_m^S}{L_m^S - B} x_n^S - \frac{B}{L_m^S - B} x_B \quad (14)$$

The last line needed to execute the McCabe-Thiele method, the feed line or q-line, where q is defined as the liquid fraction of feed, can be developed from a combined total molar balance around the column given by (15), the feed flow rate (F), an equating of the ROL and SOL (16), and mole balances at the feed stage provided by (17) and (18). Note that (16) uses the fact that at the feed point into the column, the ROL and SOL must intersect, and so one can equate and rearrange (12) and (14). The slope-intercept form for the q-line (19) allows one to solve for any vapor mole fraction (y) given liquid mole fraction (x) at the feed tray.

$$F x_F = D x_D + B x_B \quad (15)$$

$$(V_{n+1}^R - V_{n+1}^S)y = (L_n^R - L_n^S)x + D x_D + B x_B \quad (16)$$

$$L_n^R = L_n^S - qF \quad (17)$$

$$V_{n+1}^R = V_{n+1}^S + (1-q)F \quad (18)$$

$$y = -\frac{q}{1-q} x + \frac{1}{1-q} x_F \quad (19)$$

The calculation of the SOL, ROL and q-line with subsequent plotting on an underlying equilibrium diagram generates the McCabe-Thiele plot represented in Figure 2.

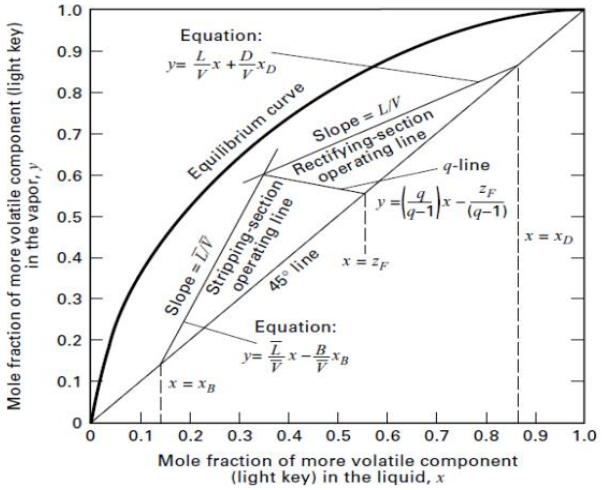

Figure 2: McCabe-Thiele plot example with rectifying and stripping section operating lines and feed-line indicated.

Experimental Procedure

Tests, measurements, and control of the distillation column was conducted through a graphical programming environment called LabVIEW [24,25]. Visual programming functions of LabVIEW enabled a controlled start-up procedure. The procedure included testing the feed tank initial concentration, and initiating heaters, coolers, and feed flow.

A first goal was to determine how reflux ratio effected the product purity. All the other inputs in the experimental procedure were fixed. The feed flow rate was to be at a fixed rate somewhere between 10 and 15 ml/min. The feed temperature was set at the saturated liquid temperature. The reboiler duty was set to 35%. The reflux percent was varied from 30% to 60% in increments of 10%.

A second goal was to determine the effect of varying flow rates on product purity. Within in each flow rate, the reflux percent was varied to attempt to maximize the purity of the product. The flow feed rate was varied from 5 to 15 ml/min. The reflux percent was varied from 30% to 80%. The temperature was also set at saturated liquid temperature. The reboiler duty was set at 35%. Data was recorded when the system was at steady state for each of the different reflux ratios.

The reboiler duty and power were changed throughout the experiments to maintain safe operating conditions. The level of the reboiler was to be above the heater and below the neck. With varying flow rates and reflux percent's, the level would get too low or high. If the level was too low, the power would be reduced or shut off to increase the level. If the level got too high, the reboiler power was increased to decrease the level.

During each experiment, mass balances were performed to make sure the system was where it needed to be. The feed flow rate was determined with a scale under the feed tank. The distillate flow was timed with a stopwatch when the flow was routed to a graduated cylinder. The bottom flow was timed to make sure flows were where they should be. On the LabVIEW software, the bottom flow was calculated by subtracting the distillate flow from the feed flow.

Material and safety information of all materials used in the experimental procedures can be found in Appendix A of the Supplementary Material.

Experimental Apparatus

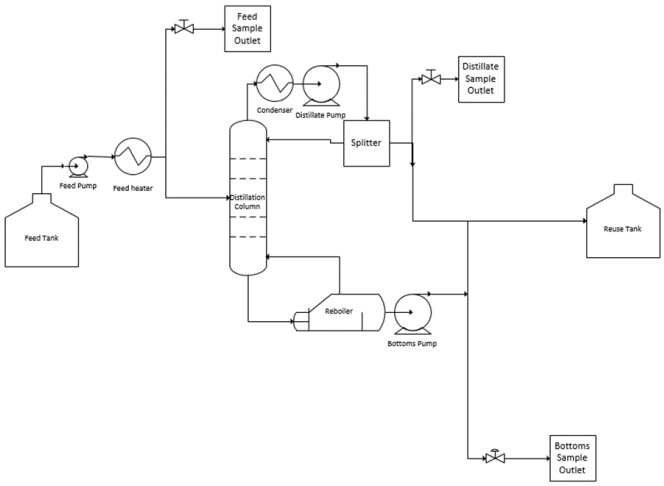

Figure 3: Process Flow Diagram for a modified Oldershaw Distillation Column.

The process flow diagram for the experimental procedure part of the work is shown in Figure 3. Starting from the feed tank the stream is sent to a pump and a heater to prepare for injection into the distillation column. Some of that stream may make a detour to a sample outlet where there is a spout and a gage for taking concentration and flow rate measurements. After going through a total condenser with a split reflux stream, the distillate is sent to the "Reuse" tank with some of it again going to a valve that connects to a sample outlet. The bottoms go through a similar path. First, the bottoms go through a partial reboiler with the vapor going back into the column. The liquid bottoms then go to the reuse tank with part of that stream heading to a valve that connects to the last sample outlet. After the shutdown process has commenced, the reuse tank is connected back to the feed tank, and the feed tank is refilled with the contents of the reuse tank.

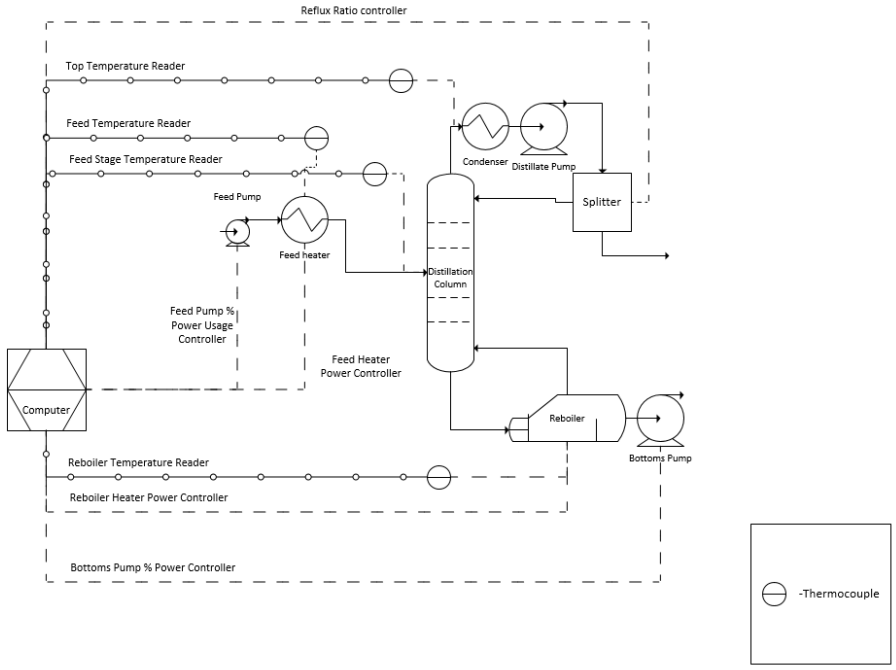

Figure 4: PID Controller Diagram for a semi-controlled modified Oldershaw distillation Column.

The control schematic in Figure 4 shows the controls that were primarily used for data collection and inspection during the experimental procedures. In this control schematic, there are four thermocouples used for monitoring the temperature of the distillate, the reboiler and bottoms, the feed, and the feed heater. The power and control to various units was controlled via LabView including the feed pump, feed heater, reboiler, and bottoms pump.

Limitation of Experimental Apparatus

There are some limitations inherent to the design of the control apparatus. The flow rate for the distillate and bottoms was not measured by the control system but instead, it was measured and input manually via a manual measurement which might have introduced error in the measurements. Similarly, the feed flow rate was measured manually. The errors could be decreased by introducing a flow rate sensor at the feed, distillation, and bottom steams. Improving the control structure for the reboiler would also increase the ability of the system to reach steady state efficiently. One way to do this would be to introduce an automatic controller instead of a manual controller to the reboiler and bottoms pump power. This controller would be connected to a level reader for the boiler to avoid dry out or flooding of the pump. This improvement would enable the avoidance of unnecessary change to the system conditions that would prolong the wait for the achieving of steady state. Also, the experimental apparatus is a smaller scale used to investigate relationships between operational variables. Changing any variable has a larger overall effect on the system's operation than the change expected on a larger scale operation. A need to account for this scale-up effect would need to be considered.

Results and Discussion

The first objective of this work was to incorporate VLE data on the IPA and MeOH binary mixture to devise an operational plan to enrich the distillate stream with MeOH. The feed MeOH volume fraction was 0.31 ± 0.02 corresponding a mole fraction of 0.46 ± 0.02, as determined from refractive index measurements (see Appendix B and C of the Supplementary Material). At an ambient pressure of 0.9857 ± 0.0001 bar, the T-x-y diagram given by Figure 3 modeled the thermodynamic state of the feed stream. From Figure 3, the feed had a temperature of 72.900 ± 0.001 °C - assumed to be a saturated liquid - and this value was used as the setpoint for the feed heater Proportional-Integral-Derivative (PID) controller.

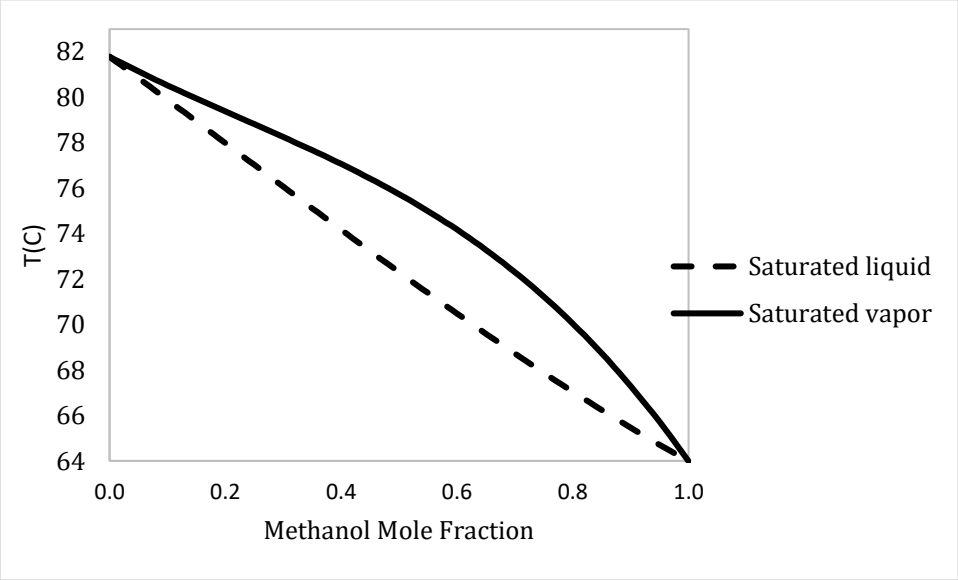

Figure 5: T-x-y diagram for IPA and MeOH binary at a pressure of 0.09857 ± 0.0001 bar. Data source is given by Table 15 in Appendix D of the Supplementary Material.

The feed for the experimental conditions remained compositionally unchanged. This, combined with a room pressure that remained within 0.001 bar, supported the assumption that the thermodynamic state of the feed remained invariant throughout the experiment. Four values of the reflux percent - 30%, 40%, 50% and 60% - which were converted to reflux ratios of 0.43, 0.67, 1 and 1.5 (see calculations in Appendix E of the Supplementary Material) were sampled to determine its effect on the purity of the distillate (measured by the mole fraction of MeOH). These values were selected to sample a broad operating envelope but to avoid excursions into unfavourable regions of reflux percent space (values below 30% and above 70%). As the reflux ratio approaches 0, reduced liquid flows down the column would promote vapor entrainment and flooding. As the reflux ratio approaches 1, weeping and dumping could result as vapor flows would be overwhelmed by the liquid. These scenarios were controlled for by judicious selection of the reflux ratios. Empirical averages of the distillate and bottoms MeOH mole fraction and flow rates for the four experimental runs are displayed in Table 1. The values from the bottoms and distillate flow columns were implemented in material balance calculations during lab to ensure that the system was approaching mass/mole balance. The calculations comprised total and species balances and were used to adjust the bottoms pump to move the system towards mass balance, see Appendix H of the Supplementary Material for the structure of these calculations and for an example calculation.

Table 1: Empirical measurements of composition are from calibrated lab refractometer. Feed flow rate was maintained at 12.44 ± 0.03 [g/min] with a MeOH mole fraction of 0.312 ± 0.02 and at a controlled temperature of 72.9 [C]. Feed, bottoms and distillate flow were calculated from volumetric flow rates by multiplying volumetric flow by the volume-fraction weighted density of the mixture. This method ignores volume change upon mixing and was performed to verify the material balance.

Reflux Ratio	MeOH Distillate Mole Fraction	MeOH Bottoms Mole Fraction	Bottoms Flow [g/min]	Distillate Flow [g/min]
0.4	0.71 ± 0.01	0.29 ± 0.04	8.16 ± 0.03	4.24 ± 0.01
0.7	0.75 ± 0.01	0.31 ± 0.04	9.01 ± 0.03	3.49 ± 0.01
1.0	0.80 ± 0.01	0.32 ± 0.03	9.52 ± 0.03	2.92 ± 0.01
1.5	0.87 ± 0.01	0.34 ± 0.03	10.16 ± 0.03	2.20 ± 0.01

The mole fraction of MeOH was observed to a be a monotonic increasing function of the reflux ratio and this was validated using a rigorous model of the distillation column on the Aspen Plus V10 process simulation software. Establishment of the simulation model consisted of an initial non-rigorous modelling using the Aspen Plus DSTWU module programmed with the input conditions given in Table 2. The DSTWU model generated the outputs stated in Table 5. As can be seen, the estimated number of theoretical trays was 11. Recall, a theoretical tray is one that satisfies the mathematical model given in Figure 1 and (6)-(10). A McCabe-Thiele diagram was formed too independently

estimate the number of theoretical trays, see Figure 6. The McCabe-Thiele method predicted 10 theoretical trays as can be observed in Figure 6. The column efficiency, calculable from (5), was found to be 50% and 55%, with number of actual trays = 20, according to the McCabe-Thiele method and Aspen Plus simulation results, respectively. Tray efficiency was estimated using the O'Connell correlation (4) and a distillate mole fraction = 0.87 and bottoms = 0.34., with MeOH and IPA viscosities of 0.543 [cP] and 2.1 [cP], respectively. The column-wise tray efficiency was estimated at 47%.

Table 2: Aspen Plus DSTWU model specifications. Values match empirical measurements from lab and were used to reconstruct distillation column model that can recapitulate empirical findings.

	Feed	Distillate	Bottoms
MeOH mole fraction	0.462	0.870	0.034
IPA mole fraction	0.522	0.130	0.966
Temperature (C)	72.9	64.8	81.2
Pressure (bar)	0.986	1.01	1.01

Table 3: DSTWU results. Note that feed stage for the laboratory column was at tray 10 whereas DSTWU returned a feed stage of 11.

Minimum Reflux Ratio (Rmin)	0.78
Actual reflux ratio (R)	1.3
Min number of stages	11
Number of actual stages	20
Feed stage	11

A graphical representation of the relationship between MeOH distillate mole fraction and the reflux ratio is exhibited in Figure 7. Product purity was predicted to increase with respect to increased values of the reflux ratio since returning cooled condensed liquid back to the top of the column would facilitate condensation of the IPA in the vapor which would prevent it from entering the overhead vapor stream. The simulation curve, see on Figure 7, was created through sensitivity analysis where a range of values for the distillate MeOH mole fraction was sampled while varying the reflux ratio. The experimental values were within error of the predicted values. Observation of the alignment between the empirical data and the RadFrac model indicates a divergence between model prediction and observation with increasing values of the reflux ratio. The experimental values demonstrated a fit to a linear equation with a coefficient of determination of 0.999. The model curve demonstrated a fit to a second order polynomial with an R^2 of 0.999. Although the mathematical form of the fit is unimportant for this experiment, the model prediction curve suggests that a maximal element, in the form of a reflux ratio and MeOH purity ordered pair whose value for MeOH is greater than all others, exists. In fact, at total reflux, when no distillate is being removed, an upper bound to the achievable product purity is reached since the number of trays is fixed – at total reflux, the number of trays is identical to the number of theoretical trays. Summarization of the agreement between predicted and observed values was completed by computing the mean-squared error (MSE) and mean absolute error (MAE), see Table 4. These comparison measures were selected since MAE is a direct distance measure between prediction and observational values and MSE is the expected value for the error (difference) between model and empirical values. Furthermore, both functions treat error direction equivalently and so random error is not discarded.

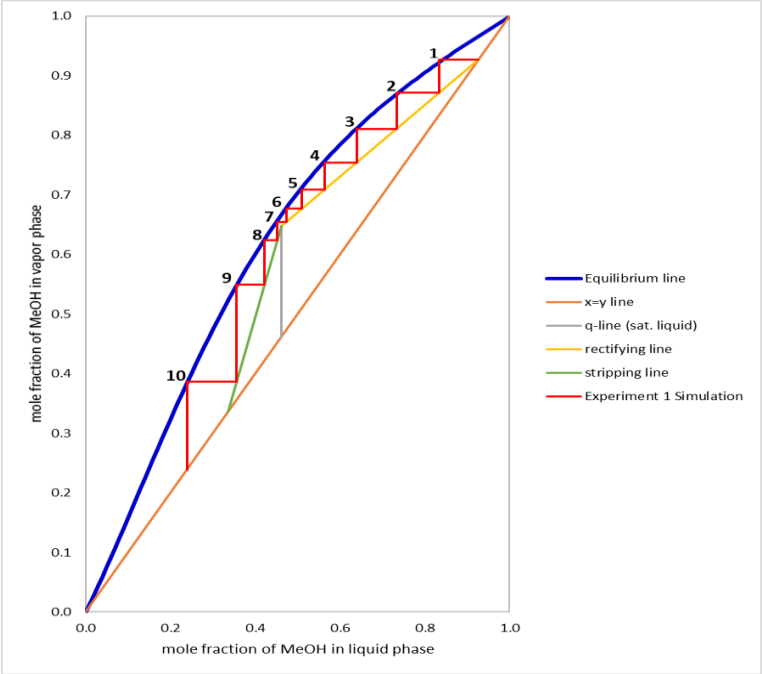

Figure 6: McCabe-Thiele plot for IPA and MeOH binary mixture separated in a modified Oldershaw column with the number of theoretical trays indicated. Specifications include a distillate mole fraction = 0.87 ± 0.01, bottoms mole fraction = 0.34 ± 0.03, feed mole fraction = 0.46 ± 0.02, ambient pressure = 0.9857 ± 0.0001 [bar], feed temperature = 72.900 ± 0.001 [C].

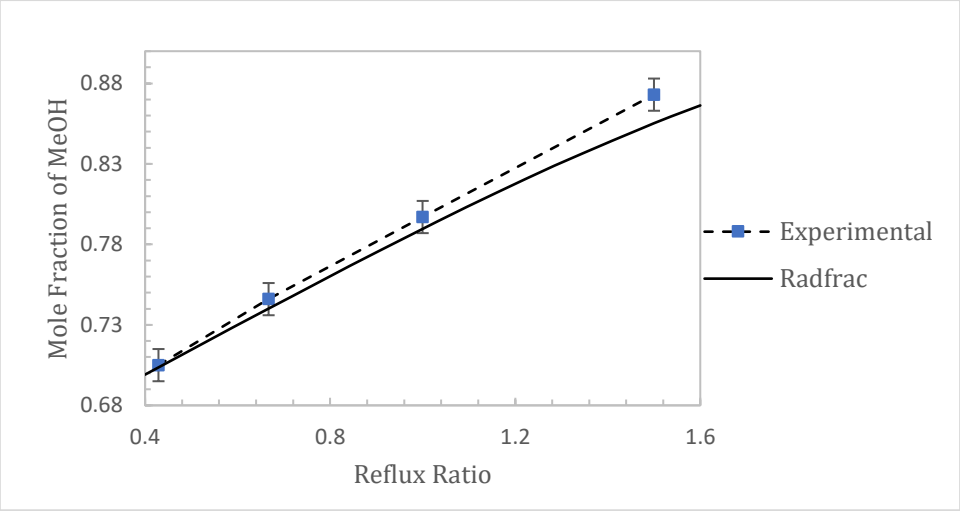

Figure 7: Plot of the relationship between MeOH mole fraction in distillate and volumetric reflux ratio. Empirical column data points were sampled at a feed flow rate of 12.44 ± 0.03 [g/min],a controlled feed termperature of 72.9 ± 0.001 [C] and ambient pressure of 0.9857 ±0.0001 [bar]. Data was gathered from the modified Oldershaw column. Mole fraction values are maxima of experimental run sequences designed to achieve steady-state system values.

Table 4: Measures of the numerical agreement between Radfrac model and lab column observations.

Reflux Ratio	MeOH Distillate Mole Fraction		Squared Error	Absolute Error
	Experimental	RadFrac		
0.4	0.71	0.70	0.0001	0.01
0.7	0.75	0.74	0.0001	0.01
1.0	0.80	0.79	0.0001	0.01
1.5	0.87	0.86	0.0001	0.01
			MSE = 0.0001	MAE = 0.01

A MAE percent of 1 and a MSE percent of 0.01 validated the high correspondence between Aspen Plus simulation predictions and the observations gathered in lab.

Determination of the relationship between the feed flow rate and product purity (MeOH mole fraction in the distillate) while controlling for the reflux ratio was pursued next. Experimental values are presented in Table 5. The feed flow rates were chosen to explore a wide operating region but also to prevent adverse events such as the tower flooding or the reboiler fluid level being depleted. It was recognized that the further a user samples from the median of the 5-15 [ml/min] interval, the greater the transit time to steady state.

Table 5: Empirical results from modified Oldershaw column with feed temperature = 72.900 ± 0.001 [C]. Feed, distillate and bottoms mass flow rates were calculated from volumetric flow rates by multiplying the volumetric flow rates by the volume-fraction weighted density of the mixture. This procedure ignores changes of volume upon mixing and was performed so as to verify the material balance.

Reflux Ratio	Feed Flow [g/min]	MeOH Distillate Mole Fraction	MeOH Bottoms Mole Fraction	Distillate Flow [g/min]	Bottoms Flow [g/min]
0.7	4.54 ± 0.02	0.72 ± 0.01	0.2 ± 0.1	2.29 ± 0.01	2.24 ± 0.03
0.7	7.42 ± 0.02	0.75 ± 0.01	0.23 ± 0.05	2.68 ± 0.01	4.77 ± 0.03
1.5	4.54 ± 0.02	0.72 ± 0.01	0.1 ± 0.1	2.25 ± 0.01	2.29 ± 0.03
1.5	7.41 ± 0.02	0.90 ± 0.01	0.25 ± 0.05	2.74 ± 0.01	5.26 ± 0.03
1.5	9.69 ± 0.02	0.87 ± 0.01	0.27 ± 0.04	2.34 ± 0.01	7.37 ± 0.03
4.0	7.42 ± 0.02	0.98 ± 0.01	0.23 ± 0.05	0.98 ± 0.01	6.44 ± 0.03

A discernment of the relationship between feed flow and product purity was a second objective. Given that the reflux ratio has an independent influence on the purity (confounding variable), it was decided to control for this interaction effect by focusing on the experimental runs that used a reflux ratio of 1.5. It can be seen in Figure 9 that the product purity of MeOH increases initially from a feed flow of 5.78 [ml/min] to a rate of 9.42 [ml/min] but then decreases from 9.42 [ml/min] to 12.33 [ml/min].

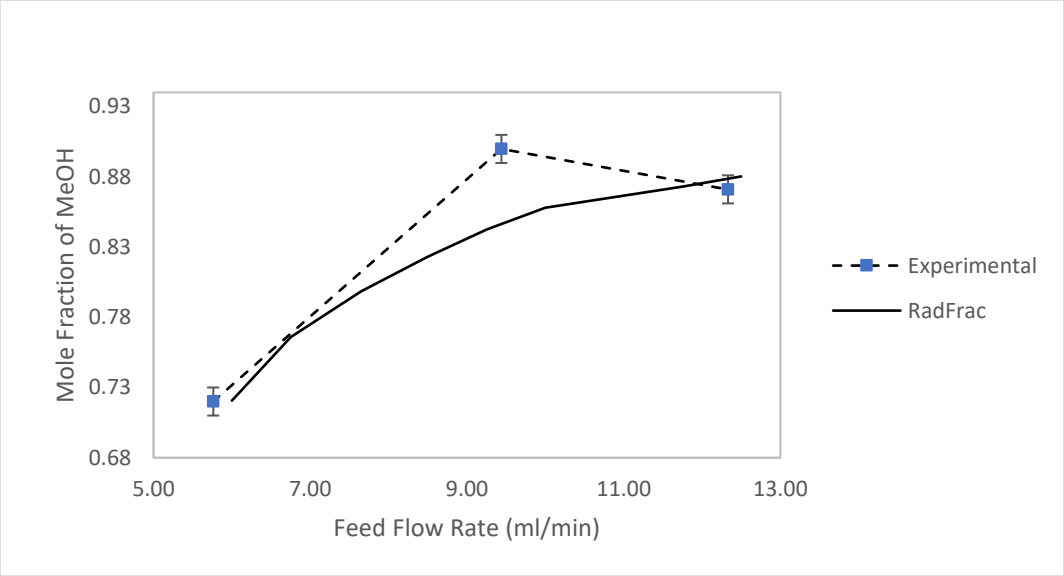

Figure 9: Plot of relationship between MeOH mole fraction in distillate and feed flow rate. Data was gathered from the modified Oldershaw column at a reflux ratio of 1.5. Feed temperature was controlled at 72.900 ± 0.001 (°C) and ambient pressure of 0.9857 bar. Mole fraction values represented the closest approximation to steady-state values for the experimental run sequences.

The comparison of the numerical agreement between the Radfrac model predictions and the empirical results was performed by computing the MAE and MSE, see Table 6.

Table 6: Measures of the numerical agreement between Radfrac model and lab column observations. Each observational record (row) was gathered at a reflux ratio of 1.5.

Feed Flow [mL/min]	MeOH Distillate Mole Fraction		Squared Error	Absolute Error
	Experimental	RadFrac		
5.78 ± 0.03	0.72	0.71	0.0001	0.01
9.42 ± 0.03	0.90	0.84	0.0036	0.06
12.33 ± 0.03	0.87	0.88	0.0001	0.01
			MSE = 0.001	MAE = 0.03

Inspection of Figure 9 reveals that Aspen Plus overpredicted the mole fraction of MeOH at the intermediate flow rate. The MAE percent was 3%, mostly due to the influence of the intermediate data point. Steady-state was never fully achieved given that the approximate volume of the column was 240 mL, so that with a flow rate of 9.42 [ml/min], 240/9.42 = 25.5 min would be an approximate residence time which can be estimated as the system time constant. Occupation of an error band ± 1% of the steady-state value demands about 5-time constants or 127.5 minutes to have elapsed. This time constraint on the experimental procedure produced experimental runs that did not exhibit MeOH mole fraction purities in the range ≥ 0.9.

In addition to the primary determination of the feed flow rate and MeOH mole fraction association, it was desired to reproduce the MeOH and reflux ratio association revealed. To do this, three reflux ratio values – 0.7, 1.5, 4.0 - were sampled at a feed flow rate of 9.40 ± 0.03 [ml/min] with results communicated in Table 5. A curve that exhibited MeOH as an increasing function of the reflux ratio was observed, see Figure 10. Furthermore, the experimental observations were within error of the simulation predictions for all but the 1.5 reflux ratio data point.

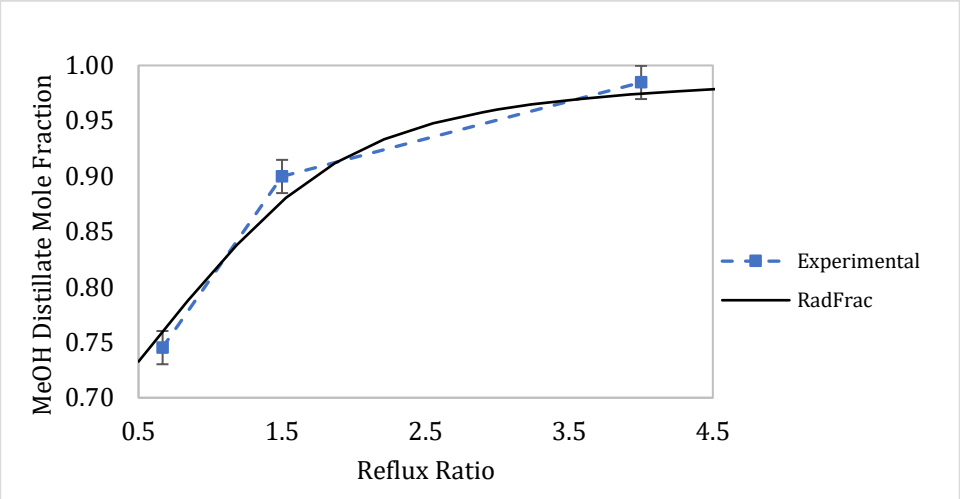

Figure 10: Plot of relationship between MeOH mole fraction in distillate and volumetric reflux ratio. Data was gathered from the modified Oldershaw column with a feed temperature controlled at 72.9 ± 0.001 (°C), an ambient pressure of 0.9857 bar and a feed flow rate of 9.42 ± 0.03 (ml/min). Mole fraction values represented the closest approximation to steady-state values for the experimental run sequences.

Design Problem

The goal for this design was to illustrate how experimental and simulation information can be utilized to design an economically feasible process for the separation of 50-50 mass percent MeOH - IPA mixture. Achieving this goal required the satisfaction of several criteria such as minimizing the total number of additional units, maximizing feed flow rate, and minimizing the amount of waste from the process. The design operates while maintaining a minimum methanol product purity of 99% and a minimum isopropanol purity of 92%. This was achieved by splitting the modular column provided into two separate columns, one for MeOH purification and the other for IPA purification, without the need for additional column segments. The use of two separate columns enabled recovery of a MeOH rich stream and an IPA stream which greatly increased the economic feasibility of the project. Although splitting the column increased the number of needed unit ops, a vastly increased profitability ensued. The second objective was achieved by examining the internal hydraulic plots generated by the distillation columns modeled by ASPEN HYSYS. The hydraulic plots were used to monitor both the weeping and entrainment capacity of each respective column, and feed flow rate, as well as distillate flow rates

and were adjusted to prevent both detrimental modes of operation within a degree of safety. The final criterion was completed through the introduction of a recycle stream that recycled a waste distillate stream that resembled the composition of the feed.

Design Process Flow Diagram

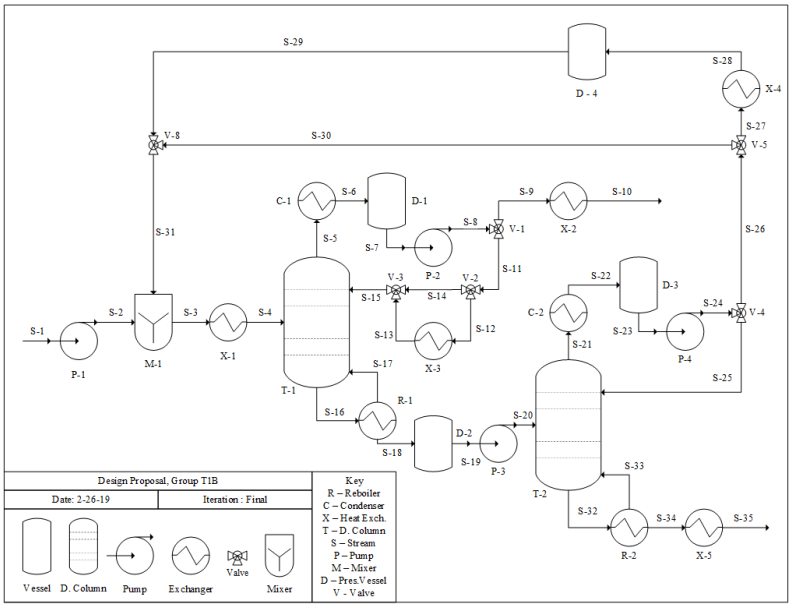

Figure 11: Process Flow DiagramUnit Overview

The process depicted in Figure 11 begins with a pump, P-1, taking feedstock, S-1, at a rate of 17.6 gallon per hour and at a composition of 49 wt. percent methanol, from a low-pressure vessel and introducing it to the mixing unit, M-1, to be mixed with waste distillate, S-38, from the second column, at the same composition and half the flow rate. Then the mixture is preheated in a boiler, X-1, to ensure that feed stream, S-4, is a saturated liquid upon entry to the first column, T-1. The column is fed at the fifth tray from the bottom, tray ten, and has a total of fifteen trays. The column then operates between 104 kPa and 115.9 kPa, with respect to the condenser and reboiler operating pressures. The first column has a distillate flow rate of 24 kilogram per hour and a reflux ratio of two. A limitation of the process was the vapor flow rate found within the rectifying section of the first column. This was due to low liquid flow rates in the rectifying section, because of low reflux flow rate, and the column feed being a saturated liquid fed at the bottom of the column. The distillate flow rate was then maximized but left within safe operating conditions to prevent entrainment of the rectifying liquid phase. Additionally, to increase liquid found in the rectifying section, the reflux was fed back as a thirty-degree subcooled liquid. This enabled a larger production rate and more pure methanol product but with an increased cooling water utility. The subsequent increase in methanol product revenue outweighed the marginal increase in cooling water cost. From the process flow diagram, the temperature of the reflux can be controlled by the unit X-3, an optional cooling unit. Determining the optimal subcooled temperature fell outside of the objectives of this investigation but could significantly decrease utility costs so should be considered as an important design consideration for future investigations. Cooler X-2 is used to cool methanol product before packaging.

The bottom product of the first column in Figure 11 is sent to an intermediate holding vessel, D-2. This vessel is setup as an oscillatory dampener between the two columns and is meant to increase stability of the system. The product is then sent to the second distillation column, T-2, that contains only five trays and operates between 114.5 kPa and 118 kPa, with respect to condenser and reboiler operating pressures. The second column is fed at the second tray from the top and was not as sensitive to distillate flow rate as the first column; therefore, sub cooling was not explored. The distillate flow rate was minimized to maximize the isopropanol bottom product flow rate, but the quality of the bottom product was hindered due to limitations of the distillate draw rate. The reflux rate for the second column was set at two just like the first column. The bottom flow rate, S-33, of the second tower is sent to a cooler, X-6, where it is cooled to a temperature around 28 degrees Celsius and sent to further packaging in stream S-36. The distillate of the second column, S-25, is sent to a splitter where 99.5% of the flow is reheated to saturation in boiler X-5, and sent back to mixer M-1 in stream S-38. The purged 0.5% is sent to a collection vessel, D-4, where it is collected along with any off-specification product produced. This vessel is a 2000-gallon storage tank. Because this tank is filled with fluid that is similar in composition to the feed it can be used as an alternative feedstock during feedstock refilling times, thus preventing any loss of time due to refilling and avoiding having to purchase another large 10000-gallon storage tank.

Economic Analysis

There were several assumptions made to ease the evaluation of the economic feasibility of the problem. The startup of the commercial application of the design was assumed to occur in partnership with a local university, The University of Kansas. The first important assumption was the selling price of methanol and isopropanol being set at $0.80 per kilogram. These prices were set from the achievable purity for each component and a cursory market research performed from online chemical wholesalers, such as Alibaba. The second assumption was that the total cost for additional units including an additional recovery system for the second column; reflux drum, condenser, reflux pump, reboiler, as well as a top and bottom for the column, a 2000-gallon vessel to hold waste feedstock, the necessary installation and cost of additional piping and instrumentation to support the acceptance of a 10000-gallon vessel, summed to a total cost of about 75,000 USD. This is a significant assumption and was based upon the average small business loan amount. It is important to note that the only major impact from this assumption is pay off time and interest rate associated with the initial startup loan. The interest rate for the 80,000 USD loan - an added 5,000 USD was needed to prevent bankruptcy in the first year - was assumed to be 12.5%. This was based upon a cursory average small business loan interest rate search. A payoff period of three years was then selected as the minimum amount of time for loan repayment. For this expedient payoff to occur, a monthly payment of 2,750 USD is needed. This allowed minimization of interest accumulation but allowed for capital to build within the company. The monthly capital accumulation of the company can be found in Appendix L of the Supplementary Material. Another assumption was the cost and disposal of cooling water of 0.004 USD per gallon. This was estimated from the Lawrence water website, with consideration given to commercial water pricing. The cost of electricity for the electric reboilers was assumed to be 0.06 per kWh. This value was taken from Westar's website, with consideration given to commercial electricity pricing. The hourly rate of pay for the group members was set at 11.50 USD per hour. This value was set to ensure an average monthly profit. Operators will also be employed by the University of Kansas and paid through an ESCROW account setup by the startup. Rent for the space at the University of Kansas was set at 2500 USD per month. A repair rate was determined to be 0.55 USD per operating hour. Packaging was set at 0.01 USD per kg of product produced.

The number of operable hours varied on a month-to-month basis. In months where students were actively using the column it was assumed that the column could be used for 14 hours a day. Two of these hours were dedicated to startup and shutdown. On the weekends and days where students do not normally have access to the column it was assumed that the column could be operated for 24 hours. Any repairs would need to be made outside of this time. Due to variable school year calendars, the number of operating hours would vary year to year but are approximately equivalent. Operators work eight and a half hour shifts during 24-hour operation and seven and a half hour shifts during partial operating days. This allows for an overlap of 30 minutes to ensure proper communication between operators. A monthly summary of operations and an operation calendar can be seen in Figure 18 in Appendix L of the Supplementary Material. Additionally, a monthly break down of the payable, productive, and operating hours can be seen in Table 16 in Appendix L of the Supplementary Material.

The primary costs for the process included the utility and salary costs. These two costs accounted for more than 50% of the total cost of the process. The utility costs for this process came out to be 11.50 USD per operational hour based on the utility consumption estimated by the ASPEN simulation. The main contributor to the utility cost is cooling water. This is due to a large amount of water needed to achieve a 30 degrees sub cooling in the first distillation column's reflux stream. An optimization of this temperature is needed to decrease this expense. The effective payrate equates to 13.01 USD per operational hour. The only method for decreasing this cost is decreasing the base rate of 11.50 USD per hour. However, this would be uncompetitive with other jobs offered by the University of Kansas. Therefore, this is the minimum salary that can be established. It could see an increase after the loan is paid after three years or the loan repayment could be decreased to increase salary if operator quality becomes an issue. Figure 12 shows percentage cost distribution associated with the process based on the 2021 calendar.

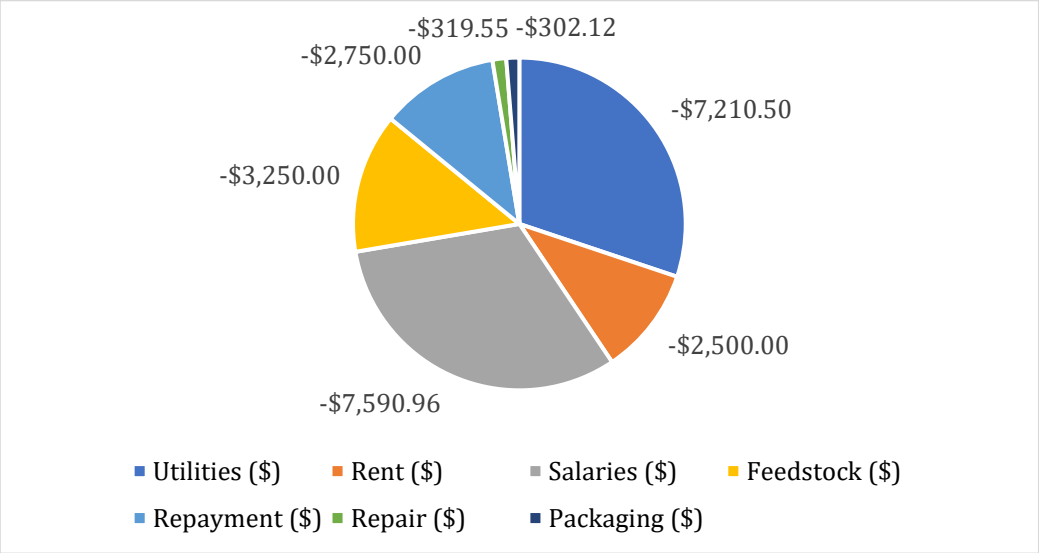

Figure 12: Distribution of costs with individual magnitudes Listed in Table 17 and 18 of Appendix L of the supplementary material.

This process design is economically feasible based on the assumptions listed above with an average monthly profit of $250. This is confirmed by the cash flow calculations shown in Tables 17 and 18 in Appendix L of the Supplementary Material. Further study in heat integration, sub cooling optimization and distillate draw optimization would further enhance the economic feasibility of the process. Ultimately, this design basis should be further explored.

Recommendations and Limitations

Several limitations existed that constrained the findings from this experiment. First, the residence time of an infinitesimally small amount of liquid, given by the ratio of the column volume (240 mL) to an average flow rate of 9 ml/min is approximately 26 min. The column can be conceived as a dynamic system under step changes to manipulated variables. Therefore, its time domain representation would be $S(1-e^{-t/\tau})$. For the system to be within 1% error of its steady state value, t must be 5τ, which would be 5 times 26 or 130 minutes. Thus, one would ideally wait 2.17 hours before acquiring data. This was not feasible with the time constraints for data collection experienced in the experimental part of this work and so some data was gathered in a system state roughly 60% of the steady state value. This suggests that transient effects were included in some of the data collection process. Second, due to the semi-automatic control configuration, the user is required to adjust the bottoms flow rate and reboiler heater power percent to control the fluid level in the reboiler. The functioning of the column has a non-zero dependency on these variables and so each change resulted in a disturbance to the system and disruption of steady state. If the system had spent 20 minutes transitioning to steady state and was disturbed by a change in the bottoms flow rate then the time to steady state would need to be restarted to ensure quality data. Again, time constraints did not permit this additional waiting time. Time restriction also prevented sampling of more data points within the operating envelope so that the identification of optimal conditions was not completed.

The main recommendation for this experiment would be to extend the data collection time so that data quality could be enhanced and more data could be gathered.

Conclusion

The formation of predictive models of distillation that have the power to explain empirical observations with small residuals is critical to forecast the operational performance of column designs. This study investigated the relationship between two column process variables – reflux ratio and feed flow rate – and the purity of MeOH in the distillate stream by operation of a modified Oldershaw column under semi-automatic control. In the first part of the experimental work, it was discovered that the MeOH mole fraction and reflux ratio were positively correlated. The MeOH mole fraction went from 0.71 ± 0.01 to 0.87 ± 0.01 in a strictly increasing fashion over the domain of reflux ratio values sampled. Simulation data from Aspen Plus's RadFrac model similarly predicted a positively monotonic function between MeOH mole fraction and reflux ratio. The percent mean absolute error (MAE) between model predictions and experimental observations was 1%. The McCabe-Thiele method and the DSTWU model from Aspen predicted the number of theoretical trays to be 10 and 11 with corresponding column efficiencies of 50% and 55%, respectively. Moreover, the tray efficiency for the column was estimated to be 49% as determined from the O'Connell correlation. In the second part of the experimental work, the predictive understanding of the column's operation was improved by demonstrating the connection between feed flow rate and MeOH mole fraction in the distillate. At a reflux ratio of 1.5, the MeOH mole fraction increased from 0.72 ± 0.01 to 0.90 ± 0.01 as the feed flow went from 5.78 ± 0.03 [ml/min] to 9.42 ± 0.03 [ml/min]. However, when the feed flow rate increased from 9.42 ± 0.03 [ml/min] to 12.33 ± 0.03 [ml/min] the MeOH decreased from 0.90 ± 0.01 to 0.87 ± 0.01. This indicated a maximum at a feed flow rate of 9.42 ± 0.03 [ml/min] for the column at a reflux ratio of 1.5. Comparison between Aspen Plus predictions and empirical

measurements resulted in a percent MAE of 3%. The strictly increasing relation between MeOH mole fraction and reflux ratio seen in the experimental work where at a flow rate of 9.40 ± 0.03 [ml/min] the MeOH mole fraction increased from 0.75 ± 0.01 to 0.98 ± 0.01 as the reflux ratio ranged from 0.7 to 4.0. The design problem sought a feasible economic solution to the separation of a 50:50 mixture of MeOH and IPA. A solution was found that consisted of sequential distillation columns that produced MeOH and IPA product streams of 99.3% and 93.6% by weight at flow rates of 24 [kg/h] and 28 [kg/h], respectively. Total capital increased at an average rate of $250/month with a peak in capital of $11,060 in August and a lower bound of $2,460 in April. This was determined to be a result of transient operating hours (operation time away from steady-state) being absent in the months of June and July because of no interruptions from chemical engineering classes. Salaries and utilities were found to be the dominant contributor to total liabilities. This study merged experimental and model information into a descriptive knowledge base that had the predictive power to inform the design of a complex separation design scheme.

Data Availability Statement
Data is available upon Request

Funding Details
There is no funding to disclose for this work.

Disclosure Statement
There are no financial or non-financial competing interests to disclose.

Bibliography

1. Kister H.Z. Distillation Design, 1st ed, McGraw-Hill, New York, 1992
2. Porter, E.A. "DISTILLATION." Thermopedia, A-Z Guide to Thermodynamics, Heat & Mass Transfer, and Fluids Enigineering. (2011).
3. U.S. Department of Energy. Hybrid Separations/Distillation Technology: Research Opportunities for Energy and Emissions Reduction" Industrial Technologies Program. 2005. https://www.energy.gov/sites/prod/files/2013/11/f4/hybrid_separation.pdf
4. Sholl, D.S., Lively, R.P. (2016) Seven Chemical Separations to Change the World. Nature, 532: 435-437
5. Kiss, A.A., Jobson, M. Gao, X. (2019) Reactive Distillation: Stepping Up to the Next Level of Process Intensification. Industrial & Engineering Chemistry Research. 58 : 5909-5918
6. Iwakabe, K., Nakaiwa, M., Hunag, K., Nakanishi, T., Rosjorde, A., Ohmori, T., Endo, A., Yamamoto, T. (2006) Energy Saving in Multicompartment Separation Using an Internally Heat-Generated Distillation Column (HIDiC). Applied Thermal Engineering. 26:1362-1368.
7. Kiss, A.A. (2013) Advanced Distillation Technologies: Design, Control, and Applications. 1st ed, John Wiley & Sons, UK
8. Biasi L., Romano A., Zemp, R., Heinkenschloss, M., Batista, F., Meirelles A. (2021) Distillation Columns with Mulitple Phase Divisions: How They Improve Thermodynamic Efficiency and Decrease Energy Consumption. Industrial & Engineering Chemistry Research 60: 15690-15705.
9. Chuang K.T., Nandakumar, K. "Tray Columns: Design." Encyclopedia of Separation Sciences. Academic Press Ltd. (2000).
10. Batista F.R.M., Follegatti-Romero L.A., Bessa L.C.B.A, Meirelles A.J.A. "Computational simulation applied to the investigation of industrial plants for bioethanol distillation." Computers & Chemical Engineering. 46. 2012
11. Koretsky M.D. Engineering and Chemical Thermodynamics. 2nd Edition. John Wiley & Sons. New York. 2013.
12. Poling B.E., Prausnitz J.M., O'Connell J.P. The Properties of Gases and Liquids. 5th Edition. McGraw-Hill. New York. 2004.
13. Halvorsen I.J, Skogestad, S. "Distillation Theory," Encyclopedia of Separation Sciences. Academic Press Ltd. (2000).
14. Elliot J.R., Lira C.T. Introductory Chemical Engineering Thermodynamics. 2nd Edition. Prentice Hall. New York. 2012
15. Alfradique M.F., Castier M. "Modeling and simulation of reactive distillation columns using computer algebra." Computers and Chemical Engineering. 2005; 29(9):1875-1884.
16. Seader, Henly. Seperation Process Principles. John Wiley & Sons. 2nd Edition, 2006. Online.
17. Steffen, V., Silva, E. "Steady-State Modeling of Equilibrium Distillation". Distillation – Innovative Applications and Modeling. InTechOpen. Edited by Marisa Mendes. 2016.
18. Li J., Lei Z., Ding Z., Li C. "Azeotropic Distillation: A Review of Mathematical Models". Separation & Purification Reviews (2005) 34:1, 87-129.
19. Alfradique M.F., Castier M. "Modeling and simulation of reactive distillation columns using computer algebra." Computers and Chemical Engineering. 2005; 29(9):1875-1884
20. McCabe, W.L., E.W. Thiele. "Graphical design of fractionating columns." Industrial & Engineering Chemsitry. 17(6); 605-611. 1925.
21. Lee J.W., Hauan S., Lien K.M., Westerberg A.W. "A graphical method for designing reactive distillation columns. II. The McCabe-Thiele method." Proc. R. Soc. Lond. A. (2000) 456: 1965-1978.
22. Kong L., Maravelias C.T. "From graphical to model-based distillation colum design: a McCabe-Thiele-inspired mathematical programming approach." AIChE Journal. 65. 2019
23. Ho T.J., Huang C.T., Lee L.S., Chen C.T. "Extended Ponchon-Savarit method for graphically analyzing and designing inernally heat-integrated distillation columns." Industrial & Engineering Chemistry Research. 49: 350-358. 2010

24. Bress, T.J. Effective LabVIEW Programming. NTS Press. 2013.
25. "LabVIEW." Base 2019. National Instruments. Austin, TX.
26. Figuerredo M.F., Guedes B.P., Araujo J.M.M, Vasconcelos L.G., Brito S.R.P. "Optimal design of extractive distillation columns – A systematic procedure using a process simulator." Chemical Engineering Research and Design, 89(3). 2011
27. Shang Yilun. "Finite-Time Scaled Consensus in Discrete-Time Networks of Agents." Asian Journal of Control. 20(6): 2351-2356. 2018.

Supplementary Material:

Appendix A: Sample Explosion, Exposure Limit Calculations, and Materials and Safety.

Methanol and isopropanol were the two chemicals used in this experiment. Chemical information can be found in Table 1 below.

Table 1: Chemical Purities and Properties

Component	Purity of Chemical	Impurities	Density (g/mL)	Boiling Point (°C)
Methanol	≥99.8%	≤0.1% Water	0.791	64.7
Isopropanol	≥99.5%	≤0.2% Water	0.785	82

Safety is one of the biggest concerns anytime working in a laboratory setting. There are eight categories of safety. These categories are chemical, flammability, temperature, pressure, electrical, sharps, slips trips and falls, and ergonomics. Both chemicals have toxicity, irritation, and organ damage potential. Both chemicals are extremely flammable, so keeping them away from ignition sources is important. With the reboiler, there are temperature concerns. The system could get hot to the touch and burn skin. Anytime a system could be closed, there is a chance for pressure buildup. There is an electrical concern with power outlets and liquids. If a vial was to break, there could be a sharps concern. There is a slips concern if a liquid is spilled on the ground. Accessing the system in the container presents and ergonomic concern. With proper personal protective equipment and safe lab practices, these safety concerns were avoided.

Methanol and Isopropanol have personal exposure limits and explosion limits displayed in Table 2 below. Sample calculations for how the limits were determined are shown in Appendix A.

Table 2: Personal Exposure Limits and Upper/Lower Explosion Limits Data

	Personal Exposure Limit		Lower Explosion Limit		Upper Explosion Limit	
Component	**ppm**	**Liquid Volume (L)**	**vol %**	**Liquid Volume (L)**	**vol %**	**Liquid Volume (L)**
Methanol	200	0.28	6	83.3	31	430
Isopropanol	400	1.05	2	52.3	12	313

In this experiment, there are personal exposure limit concerns. This considers the amount of chemical that can be spilled in the lab until it is no longer safe. Both chemicals could meet the exposure limits if the feed tank was knocked over. Methanol would reach a concern in a roughly equal mol mix for the feed sooner than isopropanol. With about 0.6 L spilled of the feed tank, methanol would be a safety concern. Safe handling of the feed tank is necessary to ensure no chemical spill.

The upper and lower explosion limits were never a concern for this experiment. The amount of liquid required to spill to be in the limits was too high. Isopropanol had the lowest limit at 52.3 L. This is significantly more than was ever accessible in this experiment.

Volume of the Lab = 35000 ft^3 = 9.911×10^8 mL

Upper Explosion Limit of isopropanol Calculation

$$Allowable\ Spilled\ Volume = \frac{Explosion\ Limit}{100} \times Volume\ of\ Lab \times \frac{Gas\ Density}{Liquid\ Density}$$

$$Allowable\ Spilled\ Volume = \frac{12}{100} \times 9.911 \times 10^8\ \text{mL} \times \frac{0.002\frac{g}{mL}}{0.785\frac{g}{mL}} \times \frac{1\ L}{1000\ mL} = 313\ L$$

Personal Exposure Limit of isopropanol Calculation

$$Allowable\ Spilled\ Volume = \frac{Exposure\ Limit\ (ppm)}{1x10^6} \times Volume\ of\ Lab \times \frac{Gas\ Density}{Liquid\ Density}$$

$$Allowable\ Spilled\ Volume = \frac{400}{1x10^6} \times 9.911 \times 10^8\ \text{mL} \times \frac{0.002\frac{g}{mL}}{0.785\frac{g}{mL}} \times \frac{1\ L}{1000\ mL} = 1.05\ L$$

Appendix B: Feed, Distillate, and Bottoms Experiment 1 IR Data

Table 9: Experiment 1 feed IR and volume fraction of methanol data with calculated uncertainties vs varying reflux ratios

Average Reflux Ratio	feed IR #1	feed IR #2	feed IR #3	feed IR avg	Feed vol frac methanol
0.4	1.360 ± 0.0005	1.360 ± 0.0005	1.360 ± 0.0005	1.360 ± 0.0005	0.312 ± 0.0005
0.7	1.360 ± 0.0005	1.360 ± 0.0005	1.360 ± 0.0005	1.360 ± 0.0005	0.312 ± 0.0005
1.0	1.360 ± 0.0005	1.360 ± 0.0005	1.360 ± 0.0005	1.360 ± 0.0005	0.312 ± 0.0005
1.5	1.360 ± 0.0005	1.360 ± 0.0005	1.360 ± 0.0005	1.360 ± 0.0005	0.312 ± 0.0005

Table 10: Experiment 1 distillate IR and volume fraction of methanol data with calculated uncertainties vs varying reflux ratios

Average Reflux Ratio	Dist IR #1	Dist IR #2	Dist IR #3	Dist IR avg	Dist vol frac methanol
0.4	1.348 ± 0.0005	1.348 ± 0.0005	1.348 ± 0.0005	1.348 ± 0.0005	0.558 ± 0.0005
0.7	1.346 ± 0.0005	1.346 ± 0.0005	1.346 ± 0.0005	1.346 ± 0.0005	0.608 ± 0.0005
1.0	1.343 ± 0.0005	1.342 ± 0.0005	1.342 ± 0.0005	1.342 ± 0.0005	0.675 ± 0.0005
1.5	1.337 ± 0.0005	1.337 ± 0.0005	1.337 ± 0.0005	1.337 ± 0.0005	0.784 ± 0.0005

Table 11: Experiment 1 bottoms IR and volume fraction of methanol data with calculated uncertainties vs varying reflux ratios

Average Reflux Ratio	Bott IR #1	Bott IR #2	Bott IR #3	Bott IR avg	Bott vol frac methanol
0.4	1.367 ± 0.0005	1.367 ± 0.0005	1.367 ± 0.0005	1.367 ± 0.0005	0.181 ± 0.0005
0.7	1.366 ± 0.0005	1.366 ± 0.0005	1.366 ± 0.0005	1.366 ± 0.0005	0.193 ± 0.0005
1.0	1.366 ± 0.0005	1.366 ± 0.0005	1.366 ± 0.0005	1.366 ± 0.0005	0.201 ± 0.0005
1.5	1.365 ± 0.0005	1.365 ± 0.0005	1.365 ± 0.0005	1.365 ± 0.0005	0.211 ± 0.0005

Appendix C: Feed, Distillate, and Bottoms Experiment 2 IR Data

Table 12: Experiment 2 feed IR and volume fraction of methanol data with calculated uncertainties vs varying feed flow rates and reflux ratios

feed flow (ml/min)	average feed flow	Average Reflux Ratio	feed IR #1	feed IR #2	feed IR #3	feed IR avg	Feed vol frac methanol
5.76 ± 0.028	5.76 ± 0.028	0.7	1.360 ± 0.0005	1.360 ± 0.0005	1.360 ± 0.0005	1.360 ± 0.0005	0.312 ± 0.0005
9.45 ± 0.028	9.45 ± 0.028	0.7	1.360 ± 0.0005	1.360 ± 0.0005	1.360 ± 0.0005	1.360 ± 0.0005	0.312 ± 0.0005
9.42 ± 0.028	9.42 ± 0.028	4.0	1.360 ± 0.0005	1.360 ± 0.0005	1.360 ± 0.0005	1.360 ± 0.0005	0.312 ± 0.0005
9.42 ± 0.028	9.43 ± 0.028	1.5	1.360 ± 0.0005	1.360 ± 0.0005	1.360 ± 0.0005	1.360 ± 0.0005	0.312 ± 0.0005
12.33 ± 0.028	12.33 ± 0.028	1.5	1.360 ± 0.0005	1.360 ± 0.0005	1.360 ± 0.0005	1.360 ± 0.0005	0.312 ± 0.0005

Table 13: Experiment 2 distillate IR and volume fraction of methanol data with calculated uncertainties vs varying feed flow rates and reflux ratios

feed flow (ml/min)	average feed flow	Average Reflux Ratio	Dist IR #1	Dist IR #2	Dist IR #3	Dist IR avg	Dist vol frac methanol
5.76 ± 0.028	5.76 ± 0.028	0.7	1.347 ± 0.0005	1.347 ± 0.0005	1.347 ± 0.0005	1.347 ± 0.0005	0.577 ± 0.0005
9.45 ± 0.028	9.45 ± 0.028	0.7	1.346 ± 0.0005	1.346 ± 0.0005	1.346 ± 0.0005	1.346 ± 0.0005	0.601 ± 0.0005
9.42 ± 0.028	9.42 ± 0.028	4.0	1.328 ± 0.0005	1.328 ± 0.0005	1.328 ± 0.0005	1.328 ± 0.0005	0.971 ± 0.0005
9.42 ± 0.028	9.43 ± 0.028	1.5	1.335 ± 0.0005	1.335 ± 0.0005	1.335 ± 0.0005	1.335 ± 0.0005	0.826 ± 0.0005
12.33 ± 0.028	12.33 ± 0.028	1.5	1.337 ± 0.0005	1.337 ± 0.0005	1.337 ± 0.0005	1.337 ± 0.0005	0.781 ± 0.0005

Table 14: Experiment 2 bottoms IR and volume fraction of methanol data with calculated uncertainties vs varying feed flow rates and reflux ratios

feed flow (ml/min)	average feed flow	Average Reflux Ratio	Bott IR #1	Bott IR #2	Bott IR #3	Bott IR avg	Bott vol frac methanol
5.76 ± 0.028	5.76 ± 0.028	0.7	1.372 ± 0.0005	1.372 ± 0.0005	1.372 ± 0.0005	1.372 ± 0.0005	0.071 ± 0.0005
9.45 ± 0.028	9.45 ± 0.028	0.7	1.368 ± 0.0005	1.368 ± 0.0005	1.368 ± 0.0005	1.368 ± 0.0005	0.146 ± 0.0005
9.42 ± 0.028	9.42 ± 0.028	4.0	1.369 ± 0.0005	1.369 ± 0.0005	1.369 ± 0.0005	1.369 ± 0.0005	0.139 ± 0.0005
9.42 ± 0.028	9.43 ± 0.028	1.5	1.368 ± 0.0005	1.368 ± 0.0005	1.368 ± 0.0005	1.368 ± 0.0005	0.151 ± 0.0005
12.33 ± 0.028	12.33 ± 0.028	1.5	1.367 ± 0.0005	1.367 ± 0.0005	1.367 ± 0.0005	1.367 ± 0.0005	0.171 ± 0.0005

Appendix D: T-x-y diagram data for figure 5

Table 15: T-x-y Data for IPA and MeOH binary mixture at a pressure of 0.09857 bar

Methanol Mole Fraction	Saturated Liquid Temperature (°C)	Saturated Vapor Temperature (°C)
0.00	56.2	56.2
0.01	56.0	56.0
0.02	55.8	55.9
0.03	55.6	55.8
0.04	55.4	55.6
0.05	55.2	55.5
0.06	55.0	55.4
0.07	54.8	55.3
0.08	54.6	55.1
0.09	54.5	55.0
0.10	54.3	54.9
0.11	54.1	54.8

0.12	53.9	54.7
0.13	53.7	54.5
0.14	53.5	54.4
0.15	53.3	54.3
0.16	53.1	54.2
0.17	52.9	54.1
0.18	52.7	54.0
0.19	52.5	53.9
0.20	52.4	53.7
0.21	52.2	53.6
0.22	52.0	53.5
0.23	51.8	53.4
0.24	51.6	53.3
0.25	51.4	53.2
0.26	51.2	53.1
0.27	51.0	53.0
0.28	50.8	52.8
0.29	50.6	52.7
0.30	50.4	52.6
0.31	50.2	52.5
0.32	50.1	52.4
0.33	49.9	52.3
0.34	49.7	52.2
Methanol Mole Fraction	Methanol Mole Fraction	Methanol Mole Fraction
0.35	49.5	52.0
0.36	49.3	51.9
0.37	49.1	51.8
0.38	48.9	51.7
0.39	48.7	51.6
0.40	48.5	51.4
0.41	48.4	51.3
0.42	48.2	51.2
0.43	48.0	51.1
0.44	47.8	50.9
0.45	47.6	50.8
0.46	47.4	50.7
0.47	47.2	50.5
0.48	47.0	50.4
0.49	46.9	50.2
0.50	46.7	50.1
0.51	46.5	50.0
0.52	46.3	49.8
0.53	46.1	49.7
0.54	45.9	49.5
0.55	45.8	49.4
0.56	45.6	49.2

0.57	45.4	49.0
0.58	45.2	48.9
0.59	45.0	48.7
0.60	44.9	48.6
0.61	44.7	48.4
0.62	44.5	48.2
0.63	44.3	48.0
0.64	44.1	47.8
0.65	44.0	47.7
0.66	43.8	47.5
0.67	43.6	47.3
0.68	43.4	47.1
0.69	43.3	46.9
0.70	43.1	46.7
0.71	42.9	46.5
0.72	42.8	46.3
Methanol Mole Fraction	Saturated Liquid Temperature (°C)	Saturated Vapor Temperature (°C)
0.73	42.6	46.0
0.74	42.4	45.8
0.75	42.2	45.6
0.76	42.1	45.4
0.77	41.9	45.1
0.78	41.7	44.9
0.79	41.6	44.7
0.80	41.4	44.4
0.81	41.3	44.2
0.82	41.1	43.9
0.83	40.9	43.6
0.84	40.8	43.4
0.85	40.6	43.1
0.86	40.5	42.8
0.87	40.3	42.5
0.88	40.1	42.3
0.89	40.0	42.0
0.90	39.8	41.7
0.91	39.7	41.4
0.92	39.5	41.1
0.93	39.4	40.7
0.94	39.2	40.4
0.95	39.1	40.1
0.96	38.9	39.8
0.97	38.8	39.4
0.98	38.6	39.1
0.99	38.5	38.7
1.00	38.4	38.4

Appendix E: Reflux Percent to Reflux Ratio Calculation

$$\frac{\left(\frac{Reflux\ Percent}{100}\right)}{\left(1-\frac{Reflux\ Percent}{100}\right)} = Reflux\ Ratio$$

$$\frac{\left(\frac{30}{100}\right)}{\left(1-\frac{30}{100}\right)} = 0.429 = Reflux\ Ratio$$

Appendix F: Material Balance Sample Equations

These are the generic equations for material balances for the entire system with F being feed molar flow rate, D being distillate molar flow rate, and B being bottoms molar flow rate. The mole fraction for a species in the system, this time methanol, will be represented by x.

$$F = D + B$$

$$Fx_F = Dx_D + Bx_B$$

For the sake of this sample calculation, the data collected for a reflux ratio of 0.4 will be used.

$$(0.46)F = \left(0.105\frac{mol}{min}\right)0.71 + \left(0.157\frac{mol}{min}\right)0.29$$

$$F = 0.262\frac{mol}{min}$$

$$Fx_F = 0.120\frac{mol}{min}$$

These are both theoretical feed flow rates. The real feed flow rate is equal to 0.264 (mol/min).

$$\%\ of\ actual\ feed\ flow\ rate = \frac{F_{theoretical}}{F_{actual}}$$

$$\%\ of\ actual\ feed\ flow\ rate = \frac{0.262\frac{mol}{min}}{0.264\frac{mol}{min}} \times 100\%$$

$$\%\ of\ actual\ feed\ flow\ rate = 99.3\%$$

Appendix G: McCabe Thiele Diagram for Experiment 2

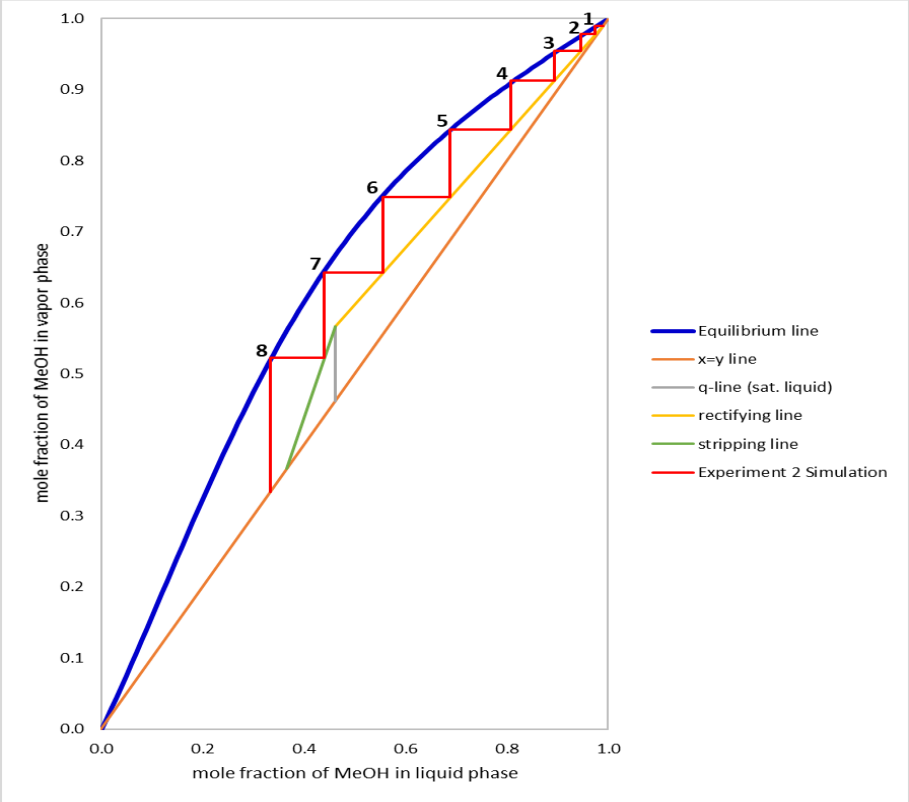

Figure 13: McCabe Thiele Diagram for experiment 2 data

Appendix H: Methanol Distillate Mole Fraction vs Reboiler Temperature Plots

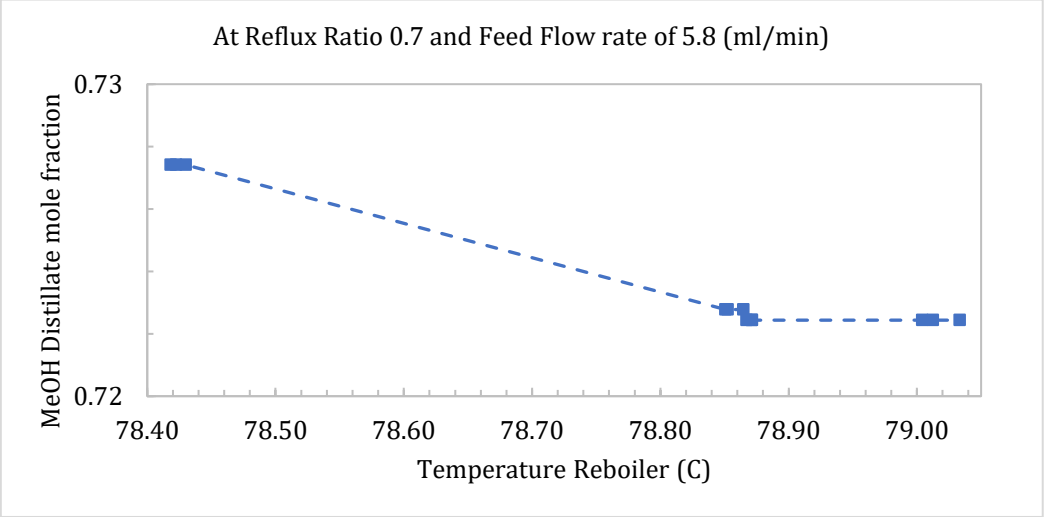

Figure 14: Methanol distillate mole fraction vs reboiler temperature at a reflux ratio of 0.7 and feed flow rate of 5.8 ml/min.

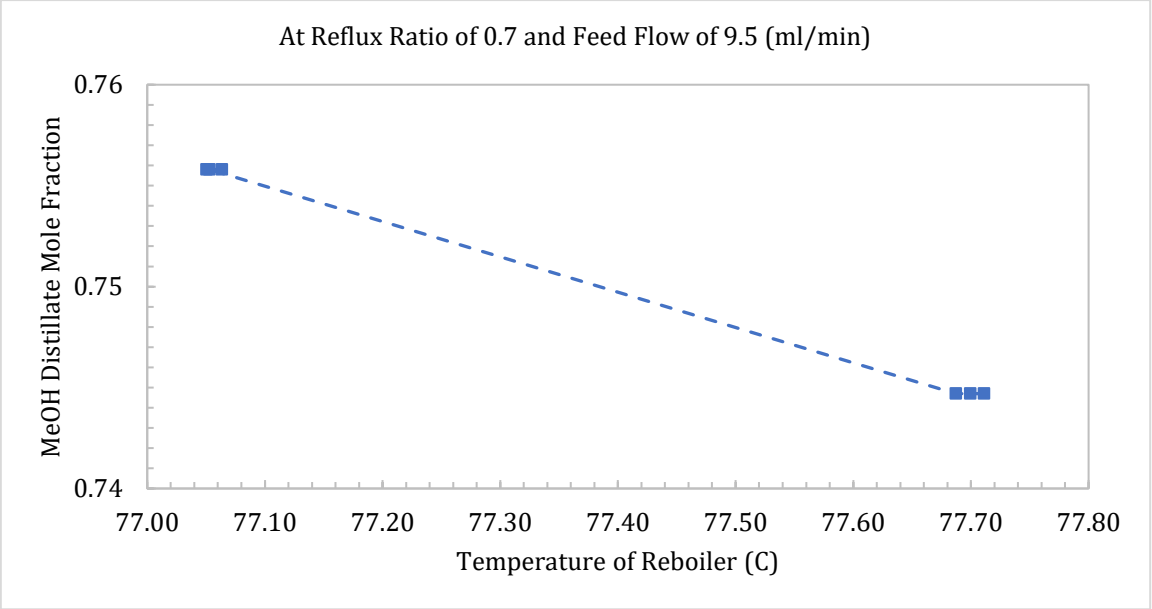

Figure 15: Methanol distillate mole fraction vs reboiler temperature at a reflux ratio of 0.7 and feed flow rate of 9.5 ml/min

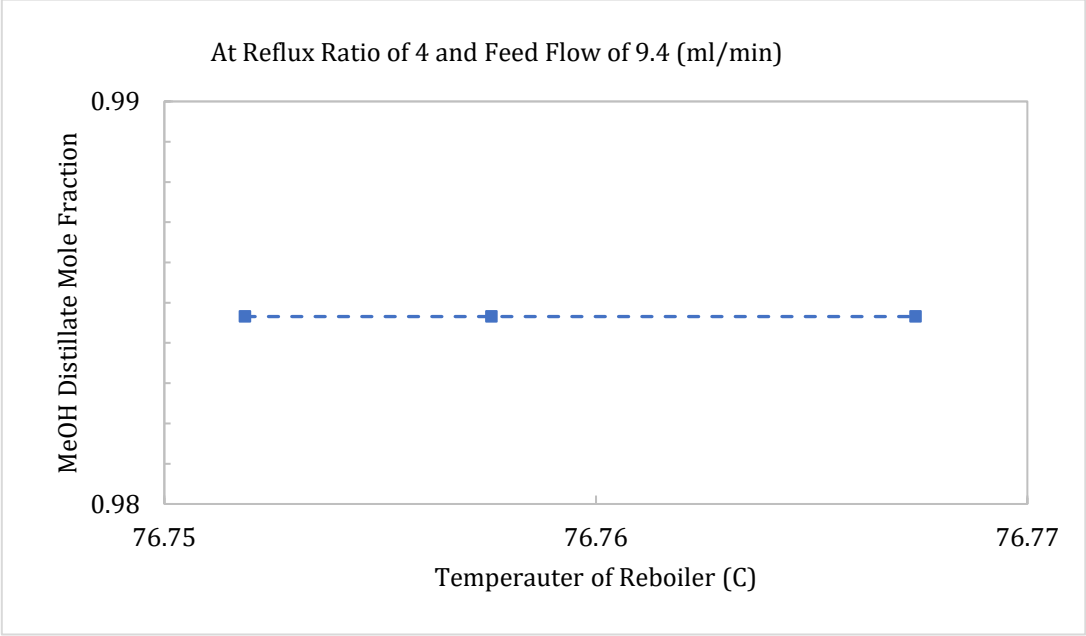

Figure 16: Methanol distillate mole fraction vs reboiler temperature at a reflux ratio of 4 and feed flow rate of 9.4 ml/min

Appendix I: Volume Fraction to Mole Fraction Calculation

$$\frac{\frac{(VF component\ 1) \times (\rho\ component\ 1)}{(MW\ component\ 1)}}{\frac{(VF\ component\ 1) \times (\rho\ component\ 1)}{(MW\ component\ 1)} + \frac{(1 - VF\ component\ 1) \times (\rho\ component\ 2)}{(MW\ component\ 2)}}$$

$$= Mole\ Fraction\ Component\ 1$$

VF = volume fraction

$\rho = density$ (g/ml)

MW = molecular weight (g/mol)

$$\frac{\frac{(0.312)\times(0.792)}{(32.04)}}{\frac{(0.312)\times(0.792)}{(32.04)}+\frac{(1-0.312)\times(0.786)}{(60.1)}}=0.462=mole\ fraction\ Methanol\ in\ feed$$

Appendix J: Error Propagation for Feed, Distillate, and Bottoms Flow Rates

Error in the feed

$$\sigma_F=\frac{\sqrt{\sigma_{mass}\sigma_{time}}}{\rho}$$

$$\sigma_F=\frac{\sqrt{0.05\ g\times 0.01\ seconds}}{0.788\ g/ml}=0.028\ ml/min$$

Error in the distillate

$$\sigma_D=\sqrt{\left(\left(\frac{1}{time}\right)(\sigma_{vol})\right)^2+\left(\left(\frac{vol}{time^2}\right)(\sigma_{time})\right)^2}$$

$$\sigma_D=\sqrt{\left(\left(\frac{1}{168.53\ seconds}\right)(0.5\ ml)\right)^2+\left(\left(\frac{15\ ml}{(168.53\ seconds)^2}\right)(0.01\ seconds)\right)^2}=0.003\ ml/min$$

Error in the bottoms

$$\sigma_B=\sigma_F+\sigma_D$$

$$\sigma_B=0.028\ ml/min+0.003\ ml/min=0.031\ ml/min$$

Appendix K: Error Propagation in Mole Fractions

$$\frac{\frac{(VF component\ 1)\times(\rho\ component\ 1)}{(MW\ component\ 1)}}{\frac{(VF\ component\ 1)\times(\rho\ component\ 1)}{(MW\ component\ 1)}+\frac{(VF\ component\ 2)\times(\rho\ component\ 2)}{(MW\ component\ 2)}}$$

$$=Mole\ Fraction\ Component\ 1$$

$$\sigma_x=\sqrt{\left(\frac{\delta f}{\delta VF_1}\sigma_{VF_1}\right)^2+\left(\frac{\delta f}{\delta VF_2}\sigma_{VF_2}\right)^2}$$

$$\frac{\delta f}{\delta VF_1}=\frac{\rho_1}{MW_1\left(\frac{\rho_1 VF_1}{MW_1}+\frac{\rho_2 VF_2}{MW_2}\right)}-\frac{(\rho_2)^2 VF_1}{(MW_1)^2\left(\frac{\rho_1 VF_1}{MW_1}+\frac{\rho_2 VF_2}{MW_2}\right)^2}$$

$$\frac{\delta f}{\delta VF_2}=\frac{-(\rho_1\rho_2 VF_1)}{MW_1 MW_2\left(\frac{\rho_1 VF_1}{MW_1}+\frac{\rho_2 VF_2}{MW_2}\right)^2}$$

$$VF_1=0.312$$

$$VF_2=0.688$$

$$MW_1=32.04\ g/mol$$

$$MW_2 = 60.1 \frac{g}{mol}$$

$$\rho_1 = 0.791\ g/ml$$

$$\rho_2 = 0.785\ g/ml$$

$$\frac{\delta f}{\delta VF_1} = 0.807$$

$$\frac{\delta f}{\delta VF_2} = -0.361$$

$$\sigma_x = \sqrt{(0.807 \times 0.0005)^2 + (-0.361 \times 0.0005)^2} = 4.42 \times 10^{-4}$$

Appendix L: Design Problem

Table 16: Monthly Schedule 2019

Month/Operation	Cont. Days	Non- Cont. Days	Prod. Hours	Payable Hours	Ops. Hours
January	23	8	648	733	678
February	8	20	432	496	504
March	15	16	552	629	612
April	8	22	456	524	534
May	24	7	660	746	687
June	30	0	720	810	720
July	31	0	744	837	744
August	26	5	684	772	702
September	9	21	468	537	543
October	8	23	468	538	549
November	9	21	468	537	546
December	22	12	672	762	705

Table 17: Cash flow for design problem

Month	Monthly Revenues	Monthly Costs						
	Products ($)	Utilities ($)	Rent ($)	Salaries ($)	Feedstock ($)	Repayment ($)	Repair ($)	Packaging ($)
January	$26,957	-$7,797	-$2,500	-$8,430	-$6,000	-$2,750	-$356	-$337
February	$17,971	-$5,796	-$2,500	-$5,704	$0	-$2,750	-$238	-$225
March	$22,963	-$7,038	-$2,500	-$7,234	-$3,000	-$2,750	-$304	-$287
April	$18,970	-$6,141	-$2,500	-$6,026	-$3,000	-$2,750	-$251	-$237
May	$27,456	-$7,901	-$2,500	-$8,579	-$3,000	-$2,750	-$363	-$343
June	$29,952	-$8,280	-$2,500	-$9,315	-$6,000	-$2,750	-$396	-$374
July	$30,950	-$8,556	-$2,500	-$9,626	-$3,000	-$2,750	-$409	-$387
August	$28,454	-$8,073	-$2,500	-$8,878	-$3,000	-$2,750	-$376	-$356
September	$19,469	-$6,245	-$2,500	-$6,176	-$3,000	-$2,750	-$257	-$243
October	$19,469	-$6,314	-$2,500	-$6,187	-$3,000	-$2,750	-$257	-$243
November	$19,469	-$6,279	-$2,500	-$6,176	-$3,000	-$2,750	-$257	-$243
December	$27,955	-$8,108	-$2,500	-$8,763	-$3,000	-$2,750	-$370	-$349
Monthly Average	$24,170	-$7,211	-$2,500	-$7,591	-$3,250	-$2,750	-$320	-$302

Table 18: Misc. cash flow for design problem

Month	Monthly Misc.			
	Profit ($)	Loans ($)	Expenditures ($)	Total Capital ($)
January	-$1,213	$80,000	-75000	$3,787
February	$759	$0.00	0	$4,546
March	-$149	$0.00	0	$4,397
April	-$1,935	$0.00	0	$2,462
May	$2,020	$0.00	0	$4,482
June	$337	$0.00	0	$4,819
July	$3,723	$0.00	0	$8,541
August	$2,522	$0.00	0	$11,063
September	-$1,702	$0.00	0	$9,361
October	-$1,782	$0.00	0	$7,578
November	-$1,736	$0.00	0	$5,842
December	$2,116	$0.00	0	$7,958
Monthly Average	$246			$6,236

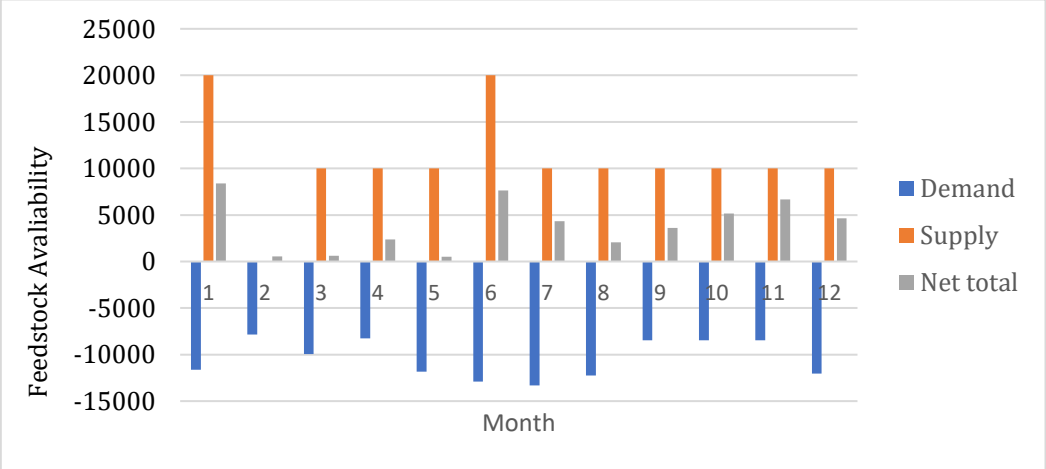

Figure 17: Feedstock avaliability for 2019.

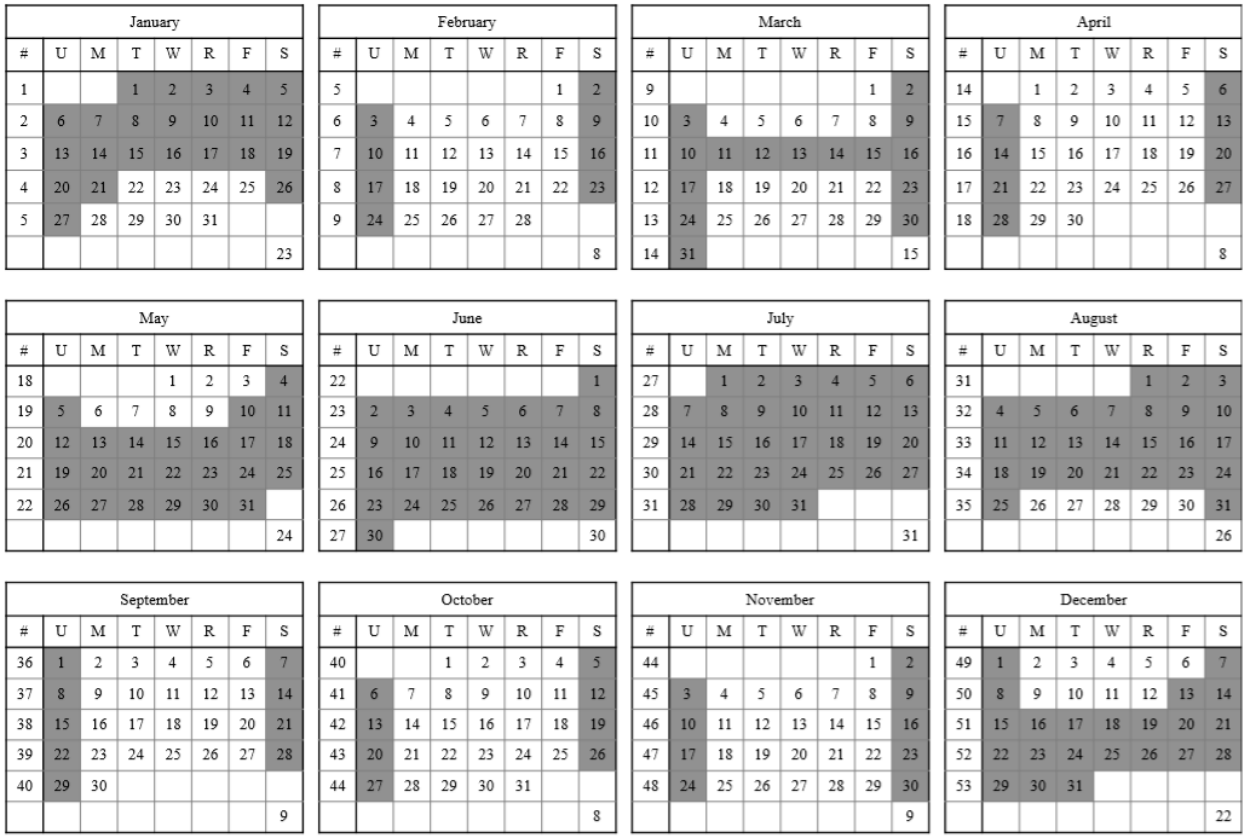

January							
#	U	M	T	W	R	F	S
1			1	2	3	4	5
2	6	7	8	9	10	11	12
3	13	14	15	16	17	18	19
4	20	21	22	23	24	25	26
5	27	28	29	30	31		
							23

February							
#	U	M	T	W	R	F	S
5						1	2
6	3	4	5	6	7	8	9
7	10	11	12	13	14	15	16
8	17	18	19	20	21	22	23
9	24	25	26	27	28		
							8

March							
#	U	M	T	W	R	F	S
9						1	2
10	3	4	5	6	7	8	9
11	10	11	12	13	14	15	16
12	17	18	19	20	21	22	23
13	24	25	26	27	28	29	30
14	31						15

April							
#	U	M	T	W	R	F	S
14		1	2	3	4	5	6
15	7	8	9	10	11	12	13
16	14	15	16	17	18	19	20
17	21	22	23	24	25	26	27
18	28	29	30				
							8

May							
#	U	M	T	W	R	F	S
18				1	2	3	4
19	5	6	7	8	9	10	11
20	12	13	14	15	16	17	18
21	19	20	21	22	23	24	25
22	26	27	28	29	30	31	
							24

June							
#	U	M	T	W	R	F	S
22							1
23	2	3	4	5	6	7	8
24	9	10	11	12	13	14	15
25	16	17	18	19	20	21	22
26	23	24	25	26	27	28	29
27	30						30

July							
#	U	M	T	W	R	F	S
27		1	2	3	4	5	6
28	7	8	9	10	11	12	13
29	14	15	16	17	18	19	20
30	21	22	23	24	25	26	27
31	28	29	30	31			
							31

August							
#	U	M	T	W	R	F	S
31					1	2	3
32	4	5	6	7	8	9	10
33	11	12	13	14	15	16	17
34	18	19	20	21	22	23	24
35	25	26	27	28	29	30	31
							26

September							
#	U	M	T	W	R	F	S
36	1	2	3	4	5	6	7
37	8	9	10	11	12	13	14
38	15	16	17	18	19	20	21
39	22	23	24	25	26	27	28
40	29	30					
							9

October							
#	U	M	T	W	R	F	S
40			1	2	3	4	5
41	6	7	8	9	10	11	12
42	13	14	15	16	17	18	19
43	20	21	22	23	24	25	26
44	27	28	29	30	31		
							8

November							
#	U	M	T	W	R	F	S
44						1	2
45	3	4	5	6	7	8	9
46	10	11	12	13	14	15	16
47	17	18	19	20	21	22	23
48	24	25	26	27	28	29	30
							9

December							
#	U	M	T	W	R	F	S
49	1	2	3	4	5	6	7
50	8	9	10	11	12	13	14
51	15	16	17	18	19	20	21
52	22	23	24	25	26	27	28
53	29	30	31				
							22

Figure 18: 2019 operation schedule. Grey indicates operation days. White indicates stop days.

Appendix M: Raw Data

Counter	Reboiler%	reflux %	feed IR#1	feed IR #2	feed IR #3	feed IR avg	feed vol frac methanol
4037	35	30	1.36026	1.36022	1.36026	1.360247	0.312023
4038	35	30	1.36026	1.36022	1.36026	1.360247	0.312023
4809	35	30	1.36026	1.36022	1.36026	1.360247	0.312023
4810	35	30	1.36026	1.36022	1.36026	1.360247	0.312023
6008	35	40	1.36026	1.36022	1.36026	1.360247	0.312023
6009	35	40	1.36026	1.36022	1.36026	1.360247	0.312023
6010	35	40	1.36026	1.36022	1.36026	1.360247	0.312023
6011	35	40	1.36026	1.36022	1.36026	1.360247	0.312023
7190	35	40	1.36026	1.36022	1.36026	1.360247	0.312023
7191	35	40	1.36026	1.36022	1.36026	1.360247	0.312023
7192	35	40	1.36026	1.36022	1.36026	1.360247	0.312023
8231	35	50	1.36026	1.36022	1.36026	1.360247	0.312023
8232	35	50	1.36026	1.36022	1.36026	1.360247	0.312023
8233	35	50	1.36026	1.36022	1.36026	1.360247	0.312023
8234	35	50	1.36026	1.36022	1.36026	1.360247	0.312023
9826	35	50	1.36026	1.36022	1.36026	1.360247	0.312023
9827	35	50	1.36026	1.36022	1.36026	1.360247	0.312023
11552	35	60	1.36026	1.36022	1.36026	1.360247	0.312023
11553	35	60	1.36026	1.36022	1.36026	1.360247	0.312023
11554	35	60	1.36026	1.36022	1.36026	1.360247	0.312023
12462	35	60	1.36026	1.36022	1.36026	1.360247	0.312023
12463	35	60	1.36026	1.36022	1.36026	1.360247	0.312023
12464	35	60	1.36026	1.36022	1.36026	1.360247	0.312023
14425	28	40	1.36026	1.36022	1.36026	1.360247	0.312023
14426	28	40	1.36026	1.36022	1.36026	1.360247	0.312023
14427	28	40	1.36026	1.36022	1.36026	1.360247	0.312023
15559	28	40	1.36026	1.36022	1.36026	1.360247	0.312023
15560	28	40	1.36026	1.36022	1.36026	1.360247	0.312023
15561	28	40	1.36026	1.36022	1.36026	1.360247	0.312023
16399	25	40	1.36026	1.36022	1.36026	1.360247	0.312023
16400	25	40	1.36026	1.36022	1.36026	1.360247	0.312023
16401	25	40	1.36026	1.36022	1.36026	1.360247	0.312023
16795	25	40	1.36026	1.36022	1.36026	1.360247	0.312023
16796	25	40	1.36026	1.36022	1.36026	1.360247	0.312023
16797	25	40	1.36026	1.36022	1.36026	1.360247	0.312023
18089	25	40	1.36026	1.36022	1.36026	1.360247	0.312023
18090	25	40	1.36026	1.36022	1.36026	1.360247	0.312023
counter	Reboiler%	reflux %	feed IR#1	feed IR #2	feed IR #3	feed IR avg	feed vol frac methanol
18091	25	40	1.36026	1.36022	1.36026	1.360247	0.312023
19162	35	40	1.36026	1.36022	1.36026	1.360247	0.312023
19163	35	40	1.36026	1.36022	1.36026	1.360247	0.312023
19164	35	40	1.36026	1.36022	1.36026	1.360247	0.312023
20736	35	80	1.36026	1.36022	1.36026	1.360247	0.312023

20737	35	80	1.36026	1.36022	1.36026	1.360247	0.312023
20738	35	80	1.36026	1.36022	1.36026	1.360247	0.312023
22216	35	60	1.36026	1.36022	1.36026	1.360247	0.312023
22217	35	60	1.36026	1.36022	1.36026	1.360247	0.312023
23950	35	60	1.36026	1.36022	1.36026	1.360247	0.312023
23951	35	60	1.36026	1.36022	1.36026	1.360247	0.312023
23952	35	60	1.36026	1.36022	1.36026	1.360247	0.312023
24379	35	60	1.36026	1.36022	1.36026	1.360247	0.312023
24380	35	60	1.36026	1.36022	1.36026	1.360247	0.312023
25261	35	60	1.36026	1.36022	1.36026	1.360247	0.312023
25262	35	60	1.36026	1.36022	1.36026	1.360247	0.312023
25400	35	60	1.36026	1.36022	1.36026	1.360247	0.312023
25401	35	60	1.36026	1.36022	1.36026	1.360247	0.312023
25402	35	60	1.36026	1.36022	1.36026	1.360247	0.312023

Dist IR #1	**Dist IR #2**	**Dist IR #3**	**Dist IR avg**	**Dist vol frac methanol**	**Bott IR #1**	**Bott IR #2**	**Bott IR #3**	**Bott IR avg**	**Bott vol frac methanol**
1.34767	1.34761	1.34759	1.347623	0.569607	1.36737	1.3673	1.36738	1.36735	0.167076
1.34767	1.34761	1.34759	1.347623	0.569607	1.36737	1.3673	1.36738	1.36735	0.167076
1.34818	1.34814	1.34819	1.34817	0.558452	1.36667	1.36671	1.36667	1.366683	0.18068
1.34818	1.34814	1.34819	1.34817	0.558452	1.36667	1.36671	1.36667	1.366683	0.18068
1.34591	1.34597	1.34599	1.345957	0.603616	1.36609	1.36617	1.36613	1.36613	0.191971
1.34591	1.34597	1.34599	1.345957	0.603616	1.36609	1.36617	1.36613	1.36613	0.191971
1.34591	1.34597	1.34599	1.345957	0.603616	1.36609	1.36617	1.36613	1.36613	0.191971
1.34591	1.34597	1.34599	1.345957	0.603616	1.36609	1.36617	1.36613	1.36613	0.191971
1.34574	1.34577	1.34571	1.34574	0.608037	1.36607	1.36609	1.36612	1.366093	0.192719
1.34574	1.34577	1.34571	1.34574	0.608037	1.36607	1.36609	1.36612	1.366093	0.192719
1.34574	1.34577	1.34571	1.34574	0.608037	1.36607	1.36609	1.36612	1.366093	0.192719
1.34259	1.34258	1.34261	1.342593	0.672246	1.36602	1.36609	1.366	1.366037	0.193875
1.34259	1.34258	1.34261	1.342593	0.672246	1.36602	1.36609	1.366	1.366037	0.193875
1.34259	1.34258	1.34261	1.342593	0.672246	1.36602	1.36609	1.366	1.366037	0.193875
1.34259	1.34258	1.34261	1.342593	0.672246	1.36602	1.36609	1.366	1.366037	0.193875
1.34251	1.34248	1.34245	1.34248	0.674559	1.36573	1.36574	1.36568	1.365717	0.200405
1.34251	1.34248	1.34245	1.34248	0.674559	1.36573	1.36574	1.36568	1.365717	0.200405
1.3377	1.33769	1.33776	1.337717	0.771756	1.36533	1.36533	1.36531	1.365323	0.208431
1.3377	1.33769	1.33776	1.337717	0.771756	1.36533	1.36533	1.36531	1.365323	0.208431
1.3377	1.33769	1.33776	1.337717	0.771756	1.36533	1.36533	1.36531	1.365323	0.208431
1.33711	1.33712	1.33715	1.337127	0.783796	1.36522	1.36517	1.36519	1.365193	0.211084
1.33711	1.33712	1.33715	1.337127	0.783796	1.36522	1.36517	1.36519	1.365193	0.211084
1.33711	1.33712	1.33715	1.337127	0.783796	1.36522	1.36517	1.36519	1.365193	0.211084
1.34698	1.34701	1.34692	1.34697	0.582938	1.37021	1.3702	1.37017	1.370193	0.109057
1.34698	1.34701	1.34692	1.34697	0.582938	1.37021	1.3702	1.37017	1.370193	0.109057
1.34698	1.34701	1.34692	1.34697	0.582938	1.37021	1.3702	1.37017	1.370193	0.109057
1.34731	1.34721	1.34722	1.347247	0.577293	1.37141	1.37137	1.37136	1.37138	0.084843
1.34731	1.34721	1.34722	1.347247	0.577293	1.37141	1.37137	1.37136	1.37138	0.084843
1.34731	1.34721	1.34722	1.347247	0.577293	1.37141	1.37137	1.37136	1.37138	0.084843
1.34729	1.34729	1.34722	1.347267	0.576885	1.37191	1.37197	1.37194	1.37194	0.073416
1.34729	1.34729	1.34722	1.347267	0.576885	1.37191	1.37197	1.37194	1.37194	0.073416

Dist IR #1	Dist IR #2	Dist IR #3	Dist IR avg	Dist vol frac methanol	Bott IR #1	Bott IR #2	Bott IR #3	Bott IR avg	Bott vol frac methanol
1.34729	1.34729	1.34722	1.347267	0.576885	1.37191	1.37197	1.37194	1.37194	0.073416
1.34729	1.34729	1.34722	1.347267	0.576885	1.3721	1.37203	1.37205	1.37206	0.070967
1.34729	1.34729	1.34722	1.347267	0.576885	1.3721	1.37203	1.37205	1.37206	0.070967
1.34729	1.34729	1.34722	1.347267	0.576885	1.3721	1.37203	1.37205	1.37206	0.070967
1.34544	1.3454	1.34543	1.345423	0.614499	1.36926	1.36927	1.36924	1.369257	0.12817
1.34544	1.3454	1.34543	1.345423	0.614499	1.36926	1.36927	1.36924	1.369257	0.12817
1.34544	1.3454	1.34543	1.345423	0.614499	1.36926	1.36927	1.36924	1.369257	0.12817
1.34619	1.34608	1.34605	1.346107	0.600555	1.3684	1.36831	1.36843	1.36838	0.146059
1.34619	1.34608	1.34605	1.346107	0.600555	1.3684	1.36831	1.36843	1.36838	0.146059
1.34619	1.34608	1.34605	1.346107	0.600555	1.3684	1.36831	1.36843	1.36838	0.146059
1.32793	1.32794	1.32793	1.327933	0.971389	1.36877	1.36868	1.36868	1.36871	0.139325
1.32793	1.32794	1.32793	1.327933	0.971389	1.36877	1.36868	1.36868	1.36871	0.139325
1.32793	1.32794	1.32793	1.327933	0.971389	1.36877	1.36868	1.36868	1.36871	0.139325
1.33508	1.33502	1.33507	1.335057	0.826035	1.36814	1.36815	1.36815	1.368147	0.15082
1.33508	1.33502	1.33507	1.335057	0.826035	1.36814	1.36815	1.36815	1.368147	0.15082
1.33727	1.33722	1.33731	1.337267	0.780939	1.36757	1.36756	1.3675	1.367543	0.163131
1.33727	1.33722	1.33731	1.337267	0.780939	1.36757	1.36756	1.3675	1.367543	0.163131
1.33727	1.33722	1.33731	1.337267	0.780939	1.36757	1.36756	1.3675	1.367543	0.163131
1.33727	1.33722	1.33731	1.337267	0.780939	1.36757	1.36756	1.3675	1.367543	0.163131
1.33727	1.33722	1.33731	1.337267	0.780939	1.36757	1.36756	1.3675	1.367543	0.163131
1.33722	1.33729	1.33724	1.33725	0.781279	1.36718	1.36712	1.36711	1.367137	0.171429
Dist IR #1	Dist IR #2	Dist IR #3	Dist IR avg	Dist vol frac methanol	Bott IR #1	Bott IR #2	Bott IR #3	Bott IR avg	Bott vol frac methanol
1.33722	1.33729	1.33724	1.33725	0.781279	1.36718	1.36712	1.36711	1.367137	0.171429
1.33722	1.33729	1.33724	1.33725	0.781279	1.36718	1.36712	1.36711	1.367137	0.171429
1.33722	1.33729	1.33724	1.33725	0.781279	1.36718	1.36712	1.36711	1.367137	0.171429
1.33722	1.33729	1.33724	1.33725	0.781279	1.36718	1.36712	1.36711	1.367137	0.171429

P (cm H2O)	**Tcond (C)**	**Tfeed heater (C)**	**Treb heater (C)**	**Ttop (C)**	**Tfeed (C)**	**Tfeed stage (C)**	**Treboiler (C)**
14.2811	21.7796	87.59892	363.1307	71.39818	72.90665	73.30903	76.29305
14.42462	21.76855	87.60704	363.1338	71.39398	72.91417	73.30403	76.30286
14.38546	21.9395	87.58488	362.9394	71.4516	72.87637	73.29463	76.15442
14.45159	21.94318	87.58406	362.9444	71.42227	72.86887	73.30046	76.17079
14.17275	22.72113	87.5947	363.041	70.62193	72.90257	73.32243	75.97702
14.57993	22.72848	87.59632	363.0509	70.59842	72.9151	73.31495	75.97947
14.35217	22.72205	87.58414	363.0551	70.61101	72.90841	73.31745	75.99258
14.24358	22.7147	87.5947	363.0557	70.56315	72.88576	73.30567	75.97198
14.56559	22.93654	87.45941	368.2669	70.58122	72.90032	73.32353	75.98382
14.46649	22.95595	87.46439	368.2607	70.56119	72.90616	73.32185	75.96087
14.61478	22.94769	87.47739	368.2461	70.55027	72.89532	73.30937	75.96743
14.90975	22.45634	87.48894	367.3586	69.46451	72.91819	73.34718	75.92598
14.78604	22.43416	87.47012	367.3464	69.41055	72.91568	73.34552	75.93253
14.90962	22.45174	87.47673	367.3403	69.41738	72.9282	73.34634	75.93499
14.86914	22.45174	87.47268	367.3342	69.40897	72.91234	73.33468	75.92598
14.54202	22.449	87.59135	365.7799	69.42834	72.8871	73.29702	75.77912

14.7352	22.45084	87.58728	365.7806	69.45442	72.89223	73.31961	75.80955
14.97047	21.82327	87.49282	366.6846	67.69475	72.87831	73.26327	75.51063
14.96753	21.83064	87.49038	366.6871	67.67872	72.8825	73.27742	75.49835
14.90561	21.82051	87.50338	366.6724	67.66015	72.89166	73.27824	75.4844
14.67884	21.89176	87.55412	365.8873	67.70439	72.898	73.29207	75.30284
14.89268	21.89176	87.55412	365.8873	67.6757	72.898	73.29123	75.3176
14.69819	21.89636	87.5476	365.8879	67.6757	72.91135	73.29622	75.30448
13.58288	21.86087	82.56267	325.8854	70.79191	72.94157	73.72178	78.42998
13.38426	21.87938	82.57343	325.8645	70.88096	72.90142	73.71834	78.42254
13.62932	21.85902	82.56595	325.8455	70.88843	72.87795	73.69744	78.41834
13.4946	21.94686	82.66873	324.8902	70.92152	72.90424	73.74444	78.85257
P (cm H2O)	Tcond (C)	Tfeed heater (C)	Treb heater (C)	Ttop (C)	Tfeed (C)	Tfeed stage (C)	Treboiler (C)
13.5321	21.96721	82.6844	324.8997	70.92917	72.90589	73.77939	78.86723
13.35034	21.94686	82.66628	324.9029	70.92235	72.92759	73.77855	78.87132
13.36045	21.94696	82.58361	310.8646	70.9216	72.92842	73.63044	79.01231
13.51238	21.95903	82.59763	310.8149	70.90324	72.90328	73.62284	79.00406
13.34718	21.95811	82.59026	310.8009	70.88142	72.91245	73.59869	79.03338
13.21222	21.85646	82.60793	307.5634	70.5755	72.89401	73.44044	78.8711
13.54004	21.86291	82.6153	307.5597	70.57383	72.87648	73.44793	78.86458
13.54972	21.86751	82.61448	307.5391	70.58221	72.88138	73.44867	78.85062
13.13878	21.63798	84.36681	305.6549	70.15103	72.90298	73.2529	77.06346
13.16951	21.62785	84.37824	305.6555	70.13759	72.89463	73.26456	77.05037
13.34729	21.64719	84.37496	305.6804	70.14263	72.89797	73.27204	77.05283
13.86495	21.41891	84.40614	368.0975	70.76509	72.94826	73.48126	77.68722
13.73477	21.45125	84.39314	368.1196	70.75426	72.90997	73.49551	77.711
13.89697	21.42168	84.39143	368.1073	70.79698	72.93907	73.47876	77.69946
14.60209	21.38934	84.26553	368.5505	64.25059	72.91885	72.12755	76.75187
14.772	21.39302	84.25246	368.5585	64.2438	72.90967	72.13338	76.75759
14.76745	21.38934	84.25408	368.5554	64.24974	72.90216	72.13254	76.76742
14.14165	21.78815	84.1814	368.7601	67.68449	72.89579	73.34647	77.17497
14.27321	21.79275	84.1863	368.7756	67.65326	72.90758	73.34658	77.20205
14.50715	21.54291	85.61204	368.8653	67.76944	72.90464	73.3037	76.5882
14.45497	21.54107	85.62263	368.842	67.74075	72.90131	73.31202	76.59148
14.4062	21.53738	85.62508	368.8457	67.734	72.90381	73.31286	76.5923
14.43765	21.3728	85.48837	368.8542	67.72163	72.88212	73.29537	76.49491
14.3701	21.37372	85.48431	368.8481	67.71656	72.88879	73.30203	76.48427
14.46891	21.60637	85.61768	369.2964	67.76092	72.88337	73.2808	76.43312
14.49082	21.59153	85.60291	369.3032	67.73888	72.89174	73.2808	76.44213
14.33511	21.56646	85.57989	369.1117	67.7387	72.91853	73.26926	76.45697
14.51468	21.57106	85.58152	369.1068	67.71339	72.92188	73.27175	76.46352
14.39407	21.59327	85.60934	369.0804	67.70672	72.89673	73.27747	76.44213